

OCT Segmentation Survey and Summary Reviews and a Novel 3D Segmentation Algorithm and a Proof of Concept Implementation

Serguei A. Mokhov^{1,2}

¹Tsinghua University, Beijing, China

²Concordia University, Montreal, QC, Canada

Yankui Sun¹

¹Tsinghua University, Beijing, China

Revision: 1.34 : Date: 2012/06/09 01:57:54

Abstract

We overview the existing OCT work, especially the practical aspects of it. We create a novel algorithm for 3D OCT segmentation with the goals of speed and/or accuracy while remaining flexible in the design and implementation for future extensions and improvements. The document at this point is a running draft being iteratively “developed” as a progress report as the work and survey advance. It contains the review and summarization of select OCT works, the design and implementation of the OCTMARF experimentation application and some results.

Contents

1 Objectives and Motivation	4
2 Literature Review	4
2.1 Background Review Papers	4
2.2 2D Segmentation Papers	5
2.3 3D Segmentation Papers	5
3 The Work of Sun et al. at Tsinghua	8
3.1 Previous Results	8
3.2 Data Description	9
4 New Algorithm	14
5 Design and Implementation	15
5.1 Language	15
5.2 Architecture	17
5.3 Data Structures	17
5.4 Data Management	18
5.5 APIs	18
5.5.1 Internal	18
5.5.2 External	19
6 Experiments	20
References	21
A Proof-of-Concept Code Excerpts	26
A.1 AScanLoader	26
A.2 Volume	28
A.3 OCTMARFApp	30
A.4 PPMDumper	47
Index	50

List of Figures

1 Synthesized from Fuller et al. (2007)	6
2 Synthesized RPE Detection from Fabritius et al. (2009)	8
3 Synthesized ILM Detection from Fabritius et al. (2009)	9
4 High-Level Algorithm for Fast 9-Layer 3D Segmentation by Yang et al. (2010) . .	10
5 Overall algorithm by Ghorbel et al. (2011)	10
6 Synthesized Preprocessing from Ghorbel et al. (2011)	11
7 Synthesized HRC Detection from Ghorbel et al. (2011)	11
8 Synthesized ILM Localization from Ghorbel et al. (2011)	11
9 Synthesized Photoreceptor (IS-OS) Segmentation from Ghorbel et al. (2011) . . .	12
10 Synthesized Alignment/Clivus Detection from Ghorbel et al. (2011)	12
11 Synthesized Inner Layers Segmentation from Ghorbel et al. (2011)	13

12	Sun et al. Some Segmentation Results	14
13	Building Our Novel Algorithm	16
14	Preliminary Project Layout	17
15	Test of Loading Provided Data in PPM To Match Provided	18
16	Test of Rudimentary Processing via Threshold	19
17	2D Zhang-Suen Skeletonizing near Fovea	20
18	2D Zhang-Suen Skeletonizing of Slice 90	21
19	2D Zhang-Suen Filling-Thinning-Contouring near Fovea	21
20	2D Zhang-Suen Filling-Thinning-Contouring of Slice 90	22
21	2D Zhang-Suen Filling-Thinning-Skeletonizing near Fovea	22
22	2D Zhang-Suen Filling-Thinning-Skeletonizing of Slice 90	23

1 Objectives and Motivation

Much of the work was done on 2D-segmentation of retinal layers; primarily by processing images one slice at a time. Disadvantages of this kind of method include:

1. relationship between images is not used;
2. processing time is expensive for OCT-volume data

As a result, there is more and more 3D segmentation research. Thus, the objectives of this work include the review the related work and a proposal of new scheme to segment retinal scans. do some PoC experiments.

2 Literature Review

This is an overview of the prominent papers in the OCT to comprise the literature review. Some of the specific papers reviewed are Yang et al. (2010); Ghorbel et al. (2011); Fabritius et al. (2009); Fuller et al. (2007); Datta et al. (2010a), and others based on their practical aspects. What follows are either citations or their summary descriptions in a common algorithmic form with the purpose of practical realization in a framework or comparative studies later on.

2.1 Background Review Papers

- The original invention of OCT is documented in Huang et al. (1991).
- Wolfgang Drexler and James G. Fujimoto. State-of-the-art retinal optical coherence tomography. *Progress in Retinal and Eye Research*, 27:45–88, 2008
- One of the recent student survey papers on the OCT – Datta et al. (2010a); in 8 IEEE pages it discusses the recent (prior and including 2010) approaches to the OCT image processing. The authors first discuss in detail the OCT technology from image acquisition hardware and software perspectives, applications, visualization, followed by the survey of the segmentation literature covering de-noising (speckle noise removal, including media filters, wavelets, ZAP, nonlinear, diffusion filters, 7x5 mean filter) and analysis (RFE high reflectivity, Markov boundary models, coherence matrix, peak and valley analysis in A-scans, adaptive thresholding, various multi-step approaches, active contours, optimal 3D graph search, random contour based analysis, support vector machines (SVM), deformable fluid-filled models). It is very well illustrated. The authors touch on some of the papers we have also briefly reviewed below, such as Fuller et al. (2007); Fabritius et al. (2009). We also have on our list of references intersecting with theirs Huang et al. (1991); Koozekanani et al. (2001); Ishikawa et al. (2005); Fernández et al. (2005); Baroni et al. (2007b); Drexler and Fujimoto (2008), which is maybe easier to refer to Datta et al. (2010a)'s summary instead for. The authors also highlight the areas that still need more work in the OCT image processing back in 2010, in particular in automation, and some errors in algorithms proposed by various authors not being able to cope with either healthy or diseased eyes, problems introduced by de-noising (decrease in speed and information loss) Some of their concerns have been answered to a degree by newer works published later in 2010 and 2011 and some of which we reviewed in Yang et al. (2010); Ghorbel et al. (2011). Datta et al. (2010a) themselves do not offer newer algorithms in that paper to solve some of the highlighted problems.

2.2 2D Segmentation Papers

This is a representative list of the 2D segmentation works that we have not reviewed in much detail in here, but provide for reference to the reader. Additional summary reviews may be added at a later date.

- Dara Koozekanani, Kim Boyer, and Cynthia Roberts. Retinal thickness measurements from optical coherence tomography using a markov boundary model. *IEEE Transactions on Medical Imaging*, 20(9):900–916, 2001
- Delia Cabrera Fernàndez, Harry M. Salinas, and Carmen A. Puliafito. Automated detection of retinal layer structures on optical coherence tomography images. *Optics Express*, 13(25):200–216, 2005
- Hiroshi Ishikawa, Daniel M. Stein, Gadi Wollstein, Siobahn Beaton, James G. Fujimoto, and Joel S. Schuman. Macular segmentation with optical coherence tomography. *Investigative Ophthalmol. Visual Scie.*, 46:2012–2017, 2005
- M. Mujat, R. C. Chan, B. Cense, B. H. Park, C. Joo, T. Akkin, T. C. Chen, and J. F. de Boer. Retinal nerve fiber layer thickness map determined from optical coherence tomography images. *Opt. Express*, 13:9480–9491, 2005
- M. Szkulmowski, M. Wojtkowski, B. Sikorski, T. Bajraszewski, V. J. Srinivasan, A. Szkulmowska, J. J. Kaluzny, James G. Fujimoto, and A. Kowalczyk. Analysis of posterior retinal layers in spectral optical coherence tomography images of the normal retina and retinal pathologies. *J. Biomed. Opt.*, 12, 2007
- Maurizio Baroni, Pina Fortunato, and Agostino La Torre. Towards quantitative analysis of retinal features in optical coherence tomography. *Med. Engin. Phys.*, 29:432–441, 2007b
- D. R. Chittajallu, G. Brunner, U. Kurkure, R. P. Yalamanchili, and I.A. Kakadiaris. Fuzzy-Cuts: A knowledge-driven graph-based method for medical image segmentation. In *Proceedings of the IEEE Conference on Computer Vision and Pattern Recognition (CVPR)*, 2009, pages 715–722. IEEE, August 2009. ISBN 978-1-4244-3991-1. doi: 10.1109/CVPR.2009.5206623
- Delia Cabrera Debuc, Harry M. Salinas, and Sudarshan Ranganathan. Improving image segmentation performance and quantitative analysis via a computer-aided grading methodology for optical coherence tomography retinal image analysis. *Journal of Biomedical Optics*, 15(4):484–496, 2010
- Yazdanpanah Azadeh, Ghassan Hamarneh, and Benjamin R. Smith. Segmentation of intra-retinal layers from optical coherence tomography images using an active contour approach. *IEEE Tran. On Medical Imaging*, 30(2):484–496, February 2011. doi: 10.1109/TMI.2010.2087390

2.3 3D Segmentation Papers

This section lists majority of the review summaries in the 3D segmentation area.

- Fuller et al. (2007) (a follow up work on the author's first attempt in Zawadzki et al. (2007)) propose the use of the support vector machines (SVMs) and machine learning to do the segmentation of a 3D volume. The approach is interactive and involves comprehensive visualization. A 3D volume is constructed and the clinicians interact with it by placing control points at the layers of interest and then the system interpolates in between. These become them the input to the SVN to learn and further segment retina scans in 3D. In this latest approach of the authors a multi-resolution imaging is used of the same area of interest in order to combat speckle noise and improve overall precision. The run-times are approx. within the range 15-30 minutes depending on the hardware. This is a good example of a machine learning segmentation, that claims to do better than neural networks, etc. but it also requires interactive user sessions before it can classify reliably the retina layers. The summary is in Figure 1.

```

1 Load 3D OCT scan and visualize;
// Interactive step by clinicians
2 Specify vertices of interest for each layer;
3 begin
4   Location of the voxel in the 3D volume:  $p_i(x_i, y_i, z_i)$ ;
5   Scalar intensity at  $p_i$ :  $f_i$ ;
6    $p_i$ 's neighbors:  $N = \{i \pm 1, j \pm 1, k \pm 1\}$ ;
7   Mean intensity value of  $p_i$ 's neighbors:

$$\bar{f}_i = \frac{1}{|N|} \sum_{n \in N} f_n$$

8   ;
8   Variance around  $p_i$ :

$$\sigma_i^2 = \frac{1}{|N|} \sum_{n \in N} [f_n - \bar{f}_i]^2$$

9   ;
9   Gradient around  $p_i$ :

$$\nabla \bar{f}_i = \frac{1}{|N| + 1} \left\{ \nabla f_i + \sum_{n \in N} \nabla f_n \right\}$$

10  ;
10 end
11 Interpolate;
12 Perform 4-fold multi-resolution image split;
13 Interpolate the layer points for each resolution;
14 Machine-learn the points using kernel-based SVN using features such as gradient,
    intensity, variance, and spacial coordinates;
15 Classify and measure layer thickness;
```

Figure 1: Synthesized from Fuller et al. (2007)

- Zongqing Lu, Qingmin Liao, and Fan Yang. A variational approach to automatic segmentation of RNFL on OCT data sets of the retina. In *16th IEEE International Conference on Image Processing*, volume 1–6, pages 3309–3312, November 2009
- From roughly the same people Garvin et al. (2008), and Garvin et al. (2009) on 3D OCT.
- Review for practical aspects: Fabritius et al. (2009). The authors automatically cover 2 layers: ILM and RPE, but they do it across the entire 3D volume. It seems they are pretty fast in most of their iterative algorithms where the number of iterations is configurable and serves as a trade off between quality of the segmentation and speed. Claimed speeds on a PC range between 16s to 21s. The ILM classification in particular is worth building upon. They use signal intensity variation based segmentation; no denoising on both healthy and diseased retinas. The algorithmic summary is in Figure 2 and Figure 3. Their RPE and ILM can be done in parallel, so speeding up the overall performance on parallel and distributed architectures.
- V. Kajic et al. Robust segmentation of intraretinal layers in the normal human fovea using a novel statistical model based on texture and shape analysis. *Optics Express*, 18(14), 2010
- M. Mujat, R. C. Chan, B. Cense, B. H. Park, C. Joo, T. Akkin, T. C. Chen, and J. F. de Boer. Retinal nerve fiber layer thickness map determined from optical coherence tomography images. *Opt. Express*, 13:9480–9491, 2005
- This work of Yang et al. (2010) uses **gradient information** to get 9 layers; they are fast and thorough, but the paper omits a few algorithm details. The first author is from Topcon, the maker of the OCT 1000 imaging hardware. Subjects – 38 (19 healthy and 19 glaucoma), including live and dead tissue. The results are compared to 4 experts' manual segmentation.

The parts of algorithm include two steps – Canny edge detection (customized with 3 thresholds, graph-based node cost assignment, dynamic programming (during the shortest path search)). The gradient aspect seems useful and fast.

The summary in the algorithm-like notation is in Figure 4.

- Rupsa Datta, S. Aditya, and D. N. Tibrewala. Advancement in OCT and image-processing techniques for automated ophthalmic diagnosis. In *Proceedings of the 2010 IEEE Students' Technology Symposium*, pages 26–33. IEEE, April 2010b. ISBN 978-1-4244-5974-2
- The result Ghorbel et al. (2011) of is also on 3D using similar equipment to Yang et al. (2010) and 8 layers using a different approach. The paper is very detailed in the algorithms used. The authors use active contours, Markov random fields, Kalman filters.

The authors don't seem to claim speed. Denoising is in play. Very detailed literature review. They have a lot larger database of 700 images (but only on healthy subjects) and test their approach from two separate imaging hardware types: Topcon's 3D OCT 1000 and Spectralis HRA+OCT(Heidelberg) and 5 experts vs. 4 in Yang et al. (2010).

The methods in Fabritius et al. (2009); Yang et al. (2010) may be more practical.

```

// Preprocessing is not done, but can be done if wanted
// RPE identification
1 begin
    // x -- width, z -- height, y -- depth in slices (B-scan)
2 Determine coordinates of max. intensity  $\max(I_{x,y}(z))$  pixels  $z_{\max(I)}(x, y)$  across
volume on  $(x, y)$ ;
3 Obtain 2D RPE position matrix  $z_{\max(I)}(x, y) = z_{rpe1}(x, y)$ ;
// Takes care of the speckle noise from RNFL
4 Using Otsu method, binarize to get erroneous pixels mask  $B_{rpe1}(x, y)$  for RPE
position matrix in  $(x, y)$  using top-hat filtering using structuring element  $5 \times 5$  pixels;
5 Replace erroneous pixes with values from nearest neighbors in  $(x, y)$ ;
6 begin
    // Set expected erroneous pixels' value to NaN
7     if  $B_{rpe1}(x, y) = 0$  then
8         |  $z_{rpe1}(x, y) = \text{NaN}$ ;
9     end
10     $Z_{rpe1}(x, y) = \text{forall the } z_{rpe1}(x, y) = \text{NaN} \text{ do}$ 
11        |  $z_{rpe1}(x, y) = \text{based on the nearest neighbor value}$ ;
12        | Smooth by moving window median filter  $30(x) \times 2(y)$  pixels;
13    end
14 end
// 30 initial pixels
15  $P = \{I_{x,y}(z), z \in [Z_{rpe1}(x, y) - 10, Z_{rpe1}(x, y) + 20]\}$ ;
16 for selected number iterations do
    Extract  $P$  pixels around RPE estimation from the original 3D volume  $(x, y, z)$ ;
    Update RPE position based on the maximum intensity;
    Smooth by moving window median filter  $40(x) \times 2(y)$  pixels;
    Reduce amount of pixels  $P$  around RPE to 20, and then 10 to do
         $P = \{I_{x,y}(z), z \in [Z_{rpe2}(x, y) - 10, Z_{rpe2}(x, y) + 10]\}$  and
         $P = \{I_{x,y}(z), z \in [Z_{rpe3}(x, y) - 5, Z_{rpe3}(x, y) + 5]\}$ ;
    end
    Smooth by moving window median filter  $20(x) \times 2(y)$  pixels;
23 end

```

Figure 2: Synthesized RPE Detection from Fabritius et al. (2009)

3 The Work of Sun et al. at Tsinghua

3.1 Previous Results

Sun et al. covered various aspects of the OCT image processing and classification using earth mover distance, SVMs, providing for detection of the nacre's layer thickness and other works, e.g. Sun and Lei (2009, 2010). The most recent work in a 3D algorithm for segmentation (submitted) is by Sun and Zhang that explores position determination for ILM, RPE, and IS/OS in a 3D volume in an efficient and robust manner by determining intensity change on both sides of the boundary simultaneously and then smoothen the recovered surface using 3D intensity difference Sun and Zhang (2012). Some segmentation results are shown in Figure 12, and more are within

```

// ILM identification
1 begin
2   Calculate threshold value and binarize each B-scan slice;
3   begin
4     foreach B-Scan in data cube do
5       Extract first 5 depth (assumed noisy) pixels
6        $\{Noise_y(x, z), y \in [1, N], x \in [1, M], z \in [1, 5]\}$ ;
7       Evaluate  $5 \times M$  pixels;
8       //  $Bnoise_y(x, z)$  is binarized  $Noise_y(x, z)$  as each Threshold is
9       different
10      Threshold = 0.5% of pixels set to 0 after binarization
11       $\{\sum_{x=1}^M \sum_{z=1}^5 Bnoise_y(x, z) \leq 0.005 \times 5 \times M\}$ ;
12    end
13  end
14  Do first ILM estimation via depth position of the first zero value of each binarized
15  A-scan;
16  for number of iterations do
17    Extract 45 pixels around estimated ILM and reprocess to remove erroneous ILM
18    pixels;
19    begin
20      |  $\{S_y(x, z), y \in [1, N], x \in [1, M], z \in [Z_{ilm}(x, y) - 15, Z_{ilm}(x, y) + 30]\}$ ;
21    end
22    Smooth by moving window medial filters  $1(x) \times 25(y)$  and  $25(y) \times 1(x)$ ;
23    Binarize using intensity with the same threshold;
24    Re-estimate ILM position based on the first zero depth value of A-scans;
25    Repeat with 30 pixels,  $[Z_{ilm2}(x, y) - 3, Z_{ilm2}(x, y) + 27]$ , and filter  $10(x) \times 1(y)$ ;
26  end
27 end

```

Figure 3: Synthesized ILM Detection from Fabritius et al. (2009)

the cited work.

3.2 Data Description

Data format description from Sun et al. with the clinical OCT data provided by Shenzhen MOPTIM Imaging Technique Co., Ltd.

- Text files: ASCII-encoded pixel intensity data. These are A-scans, where each line of text corresponds to a vertical scan. There are 100 txt files. ([data.zip](#))
- Binary images: JPEG. 100 jpg files of OCT retinal scans ([pic.zip](#)) representing 100 slides of a 3D retina scan at 480x300x100 (96dpi) resolution.

Data: 480x512x128 voxels
Result: 9 segmented boundaries in 16 seconds

```

// 2-step segmentation based on gradient:
1 foreach 408x512 A-scan a of the 3D OCT Volume do Obtain gradient information;
2 begin
3     Local customized Canny main edge result with 3 thresholds;
4     begin
5         | C(i,j) = w1 · Canny(i,j) + w2 · Axial(i,j) + w3 · Others(i,j);
6     end
7     // To interpolate missing/weak gradient info (over blood vessels, etc)
8     Global axial intension gradient;
9     Apply the shortest path search to complete and optimize detection;
10    begin
11        Dynamic programming to optimize the result
12        |
13            t(i,j) = { ∞ j < 1, j > m
14                  | C(i,j) i = n
15                  | minm=j-2:j+2 (t(i-1,m)) + C(i,j) otherwise
16        |
17    end
18 end
// Nine boundary detection
19 foreach B-scan b of the 3D OCT Volume do begin
20     Preprocess the OCT image with a customized cross-correlation based alignment algorithm to realign the
21     A-scans;
22     Detect the ILM and IS/OS boundaries (the shortest path search maps of the other boundaries can be
23     restricted to successively smaller search areas);
24     Add features edge direction and pixel intensity as the additional cost to the search graph depended on the
25     boundary of interest. The edge direction is only considered as black-to-white or white-to-black;
26     Align the image further the IS/OS boundary;
27     Detect the OS/RPE and BM/Choroid boundaries;
28     begin
29         Accurately detect the OS/RPE and BM/Choroid via a smaller kernel size applied in the Canny edge
30         detector to increase the axial detection sensitivity;
31         The search graph is constructed using only Canny edge and axial intensity gradient strength, and the
32         search area is limited below the IS/OS boundary;
33     end
34     Detect IPL/INL and NFL/GCL;
35     Detect GCL/IPL within the NFL/GCL and IPL/INL boundaries;
36     begin
37         | Apply the Canny edge detector again within that area to extract the GCL/IPL boundary;
38     end
39     Detect the INL/OPL, the dark-to-bright edge between the IPL and the outer nuclear layer;
40     Detect the ELM similarly via the dark-to-bright edge;
41     // Although the detection of a single boundary may utilize the other two pre-detected neighboring
42     // boundaries to limit the shortest path search area, the intra-retinal boundaries are allowed to
43     // overlap their neighboring boundaries.
44     Smooth intra-retinal boundaries (NFL/GCL, GCL/IPL, IPL/INL, ELM, OS/RPE, BM/Choroid) using a
45     polynomial curve-fitting based technique;
46 end
47 Apply additional smoothing across frames for 3D volumes;
48 Filter the boundaries for each A-scan location with a 1D Gaussian kernel across B-scans;
```

Figure 4: High-Level Algorithm for Fast 9-Layer 3D Segmentation by Yang et al. (2010)

- 1 Preprocessing;
- 2 HRC Detection;
- 3 ILM Localization;
- 4 Photoreceptor (IS-OS) Segmentation;
- 5 Alignment/Clivus Detection;
- 6 Inner Layers Segmentation;

Figure 5: Overall algorithm by Ghorbel et al. (2011)

```

1 begin
2   Crop image to OCT data;
3   Normalize [0..1];
4   Apply non-linear diffusion filter Weickert et al. (1998);
5 end

```

Figure 6: Synthesized Preprocessing from Ghorbel et al. (2011)

```

1 begin
2   // W is the image width
3    $y_0 = W/2;$ 
4   Select pixel  $(x_0, y_0)$  as max response to avg. filter;
5   Estimate HRC thickness  $T_{HRC}$  via profile analysis;
6   Detect HRC median line;
7   begin
8     (1) Vertically smooth image  $S(x, y) = \text{apply } 1D \text{ Gaussian filter with std. deviation } \sigma = T_{HRC}/2;$ 
9     (2) // Regular median line regardless noise and blood vessels
10     $\alpha = 0.9;$ 
11    From  $(x_0, y_0)$  column-wise in both directions deduct median line iteratively from max. output of the
12      recursive low-pass filter:  $\max(C(x, y) = (1 - \alpha)S(x, y) + \alpha C(x, y \pm 1));$ 
13    (3) Localize HRC contours;
14    begin
15      Perform k-means classification ( $k = 3$ );
16      From the median line initialize active contour curve  $X(s) = [x(s), y(s)], s \in [0, 1];$ 
17      begin
18        // The active contour is used for regularization purposes
19        Set  $\alpha$  and  $\beta$  for contour tension and rigidity;
20        Compute data fidelity  $E_{Image}(X(s))$  as a spatial diffusion of the gradient of an edge map;
21        Move  $X$  within the image's spatial domain to minimize energy  $E(X):$ 
22        
$$E(X) = \int_0^1 \frac{1}{2} (\alpha|X'(s)|^2 + \beta|X''(s)|^2 + E_{Image}(X(s))) ds;$$

23      end
24    end
25  end
26 end

```

Figure 7: Synthesized HRC Detection from Ghorbel et al. (2011)

```

1 begin
2   Re-use k-means classification ( $k = 3$ );
3   foreach Image column  $c$  scanned top-bottom do begin
4     // Pick a boundary pixel  $p(c, y)$  if
5     switch Pixel do
6       case  $p = \text{first pixel of } k = 3$ 
7       case  $p \text{ above HRC}$ 
8       case  $p = \text{first pixel of } k = 2$ 
9         | Pick  $p(c, y);$ 
10        endsw
11       otherwise
12         | Don't pick  $p(c, y)$ 
13        endsw
14      endsw
15   Select 2 highest gradient  $p_l$  and  $p_r$  from the left and right parts of the image;
16   Apply edge-tracking algorithm maximizing local gradient starting from  $p_l$  and  $p_r$ ;
17   Merge resulting curves maximizing the mean gradient;
18   Refine ILM boundary by active contour;
19   Identify foveola  $F(x_F, y_F)$  where  $x$  is maximal on ILM;
20 end

```

Figure 8: Synthesized ILM Localization from Ghorbel et al. (2011)

```

1 begin
2   Apply a peak detector on the image area WRT HRC;
3   Detect and label maxima in each column to form peak lines;
4   Init IS/OS junction extraction by selecting the peak line with min distance to HRC;
5   Iterate over other peak lines WRT the current curve;
6   begin
7     | Similar mean distance to HRC without overlap;
8     | Apply active contour using detected curve to initialize to get a contiguous regular curve;
9   end
10  Detect ONL/IS boundary;
11  begin
12    foreach Column n do Apply Kalman filter with a state vector X;
13    begin
14      | Init from the peak line above IS/OS;
15      |  $X = (Intensity, Distance)$ ;
16      | // identity matrix
17      |  $F = I$ ;
18      | Prediction:  $\hat{X}(n|n - 1) = F\hat{X}(n - 1|n - 1)$ ;
19      |  $Y(n) = \max$  intensity pixel around  $\hat{X}(n|n - 1)$ ; 0 otherwise;
20      | //  $G(n)$ adjusted each iteration
21      |  $G(n) = \text{weighted Kalman filter gain for error correction}$ ;
22      | Update:  $\hat{X}(n|n) = \hat{X}(n|n - 1) + G(n)(Y(n) - \hat{X}(n - 1))$ ;
23      | Stop:  $Y(n) = 0$  for several iterations;
24      | Regularize detective ONL/IS boundary curve by active contour;
25      | if Image is of good quality then
26        |   | Apply second Kalman filter to detect OS/RPE boundary similarly to the above;
27      | else
28        |   | Apply k-means with  $k = 2$  between IS/OS and HRC;
29        |   | // Provides first estimation around RPE-ChCap inner boundary
30        |   | Estimate thickness RPE-ChCap thickness  $T_{RPE+ChCap}$ ;
31        |   | Perform local analysis of the estimated curve for  $n$ ;
32        |   | begin
33        |   |   | OS/RPE pixel's  $y$  is a first pixel of max gradient below min intensity below the IS/OS
34        |   |   | junction;
35        |   |   | Regularize detected curve by active contour;
36        |   | end
37    end
38 end

```

Figure 9: Synthesized Photoreceptor (IS-OS) Segmentation from Ghorbel et al. (2011)

```

1 begin
2   Align image by vertical column translation against outside of the RPE+ChCap;
3   Define clivus as two highest points  $x_{Cl}, y_{Cl}$  and  $x_{Cr}, y_{Cr}$  on ILM;
4   Refine foveola position as  $\max_{distance}(ONL/IS, OS/RPE)$ ;
5 end

```

Figure 10: Synthesized Alignment/Clivus Detection from Ghorbel et al. (2011)

```

1 begin
2   Model noise and spatial pixel interaction using Markov Random Field (MRF);
3   Classify with Bayesian max a posteriori (MAP) criterion to locate a label config maximizing  $P$  based on the
4   observed image intensity;
5   begin
6     // Probability of pixel intensities  $f_s$  in class  $i$ 
7     //  $\sigma_i$  -- std. deviation
8     //  $\mu_i$  -- mean
9     
$$P(f_s|w_s = i) = \frac{1}{\sqrt{2\pi}\sigma_i} e^{-\frac{(f_s - \mu_i)^2}{2\sigma_i^2}}$$
;
10    // Potts model pixel interactions  $\phi(w_s, w_t)$  in 8-connected sites  $s$  and  $t$ 
11    if  $w_s = i$  then
12      |  $\mu_{w_s} = \mu_i$ ;
13      |  $\sigma_{w_s} = \sigma_i$ ;
14    end
15     $\beta$  empirically set to balance image data term and regulation term in  $U$ ;
16    // Energy function
17
18    
$$U(w|f) = \sum_s \left[ \frac{(f_s - \mu_{w_s})^2}{2\sigma_{w_s}^2} + \ln(\sqrt{2\pi}\sigma_{w_s}) \right] + \beta \sum_{s,t} \phi(w_s, w_t)$$

19
20    Run unsupervised  $k$ -means to init labels and initialize noise params ( $\mu_i, \sigma_i$ );
21    Minimize  $U$  using Simulated Annealing repeatedly on the original, but labeled image;
22    Determine active contours from the labeled image;
23    Detect RNFL;
24    begin
25      | Apply  $k$ -means ( $k = 2$ ) to the image top around ILM;
26      | Select clusters with higher mean intensity;
27      | Deduce RNFL contours on both sides of foveola with active contours;
28    end
29    Detect ONL;
30    begin
31      |  $k = 3$ ;
32      |  $\beta = 2$ ;
33      | Apply  $k$ -means/MRF segmentation to the foveal region constrained by clivus and ILM—RNFL and
34      | ONL/IS;
35      | Deduce the ONL boundary from the labeled image;
36      | Regularize with active contours;
37    end
38    Detect INL;
39    begin
40      |  $k = 2$ ;
41      |  $\beta = 5$ ;
42      | Apply the above method on the right and left sides from foveola;
43      | Estimate location of searched boundary as  $(y_{C1}, y_{C1}/2, y_{Cr}/2, y_{Cr})$ ;
44      | Force the curve to pass at  $y_F$  between ILM and OPL/ONL;
45      | Linear interconnect the 5 points above as the first estimate;
46      foreach Column do begin
47        | Transition pixels between labels 1 and 2 and close to the first estimate are marked as the new
48        | boundary;
49        | Initialize the new boundary estimate as active contour;
50      end
51      begin
52        | Traverse column down-up;
53        | Apply the similar process between the found curve and OPL/ONL;
54      end
55    end
56  end
57 end

```

Figure 11: Synthesized Inner Layers Segmentation from Ghorbel et al. (2011)

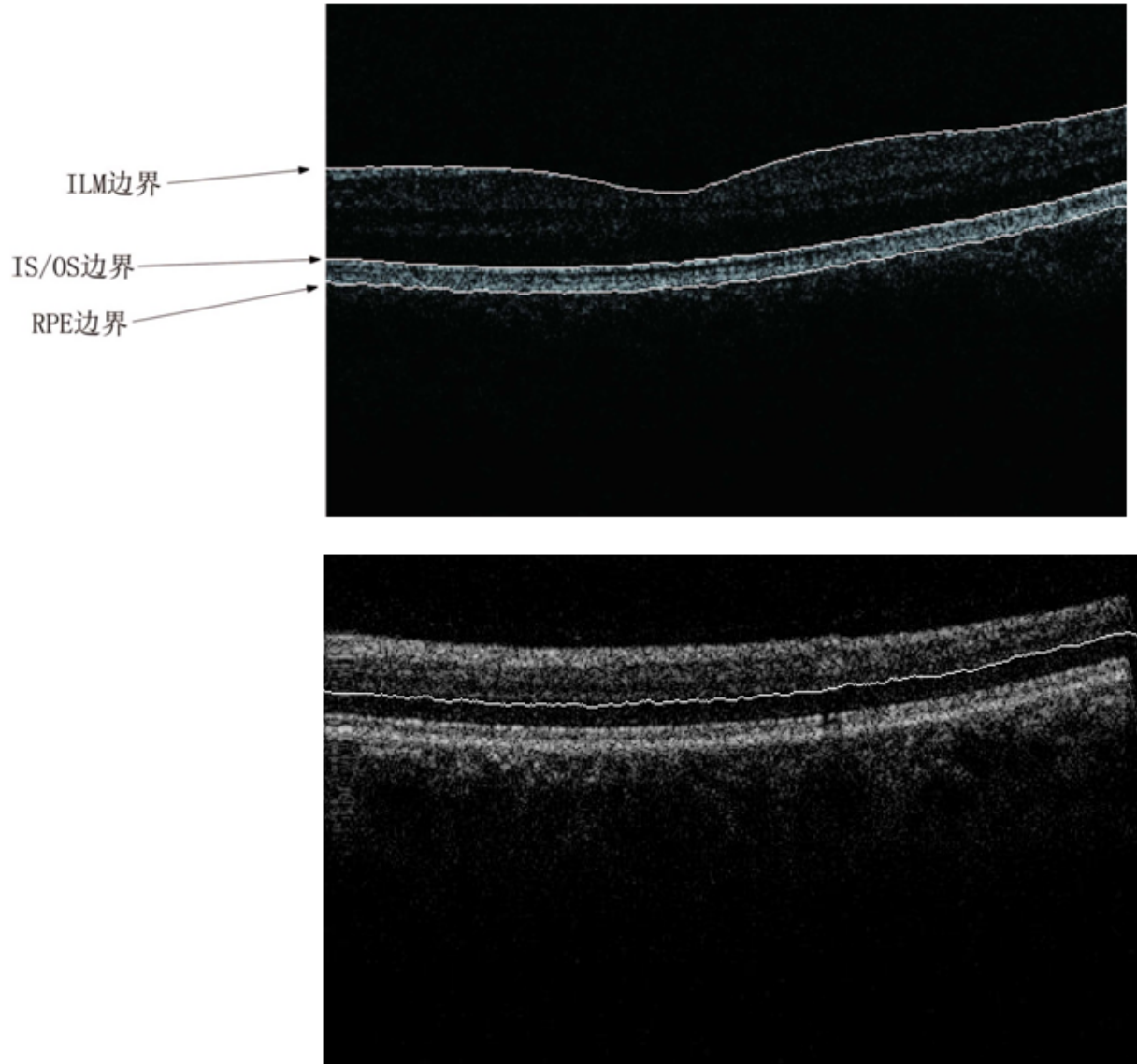


Figure 12: Sun et al. Some Segmentation Results

4 New Algorithm

This section constructs a new algorithm or a new algorithm framework derived from the reviewed literature on OCT and the previous works of authors brought into the OCT domain.

1. Use gradient, Canny edge detection.
2. **(2D done)** Apply Zhang-Suen transform to cleanse the image and skeletonize Zhang and Suen (1984). Augment the algorithm to 3D covering the nearing planes and gradient information. Use binarization before the transform per Fabritius et al. (2009).
3. Apply 3D discrete wavelet filter (dual tree) to denoise a 3D volume from Selesnick et al. (2003). Potentially borrowing from Kokare et al. (2005, 2006).

4. **(stub)** GIPSY-based The GIPSY Research and Development Group (2002–2012) distributed evaluation of OCT images.
5. Optionally re-use Neural Network (per Baroni et al. (2007a)), 2D CFE filters Haridas (2006), and machine learning implementation from MARF (some OCT papers used neural networks to classify pixels belonging to different layers.) The MARF Research and Development Group (2002–2012).
6. Optionally re-use Simulated Annealing from Cryptolysis Mokhov et al. (2005–2012a), as e.g. the authors of Ghorbel et al. (2011) use it, as per Figure 11.
7. Datta et al. (2010a) in their survey pointed out a work of Fernandez (2005) who provided a way to detect fluid-filled areas in pathological retinas using deformable models. Separately, Miao Song in her master thesis Song (2007) implemented deformable softbody simulation, where a 3D sphere of a spring-mass system is subject to inner pressure force opposed to by the spring stiffness and other external forces with collision detection. A novel idea is to use Song’s softbody to fill in the regions of each layer centered at the middles of each layer and bounded by the different intensity/gradient value pixels on the boundaries acting as collision detection points. Putting enough simulated inner pressure to the softbody object would make it fill up the layer accurately enough in real-time to define two layer boundaries for most layers for the whole 3D layer in one simulation.
8. Datta et al. (2010a) also mentioned an optimal 3D graph search by Garvin et al. in 2008 – a novel extension of this idea is to use a 3D graph with probabilities and treat the layer detection problem as a model-checking problem with probabilities instead that can be learned at 3D level with some initial training/learning. For this, there is an open-source PRISM – probabilistic model-checking tool The PRISM Team (2004–2012). A model is build for each layer with typical voxels of that layer and the corresponding graph; the probabilities are assigned based on the local and neighbors averages or medians as well as variance and gradient. Once model is build, graph is built and checked against the model.
9. Export as OBJ file format as well as 3D visualization of the entire **segmented** volume in OpenGL OpenGL Architecture Review Board (1998–2012) to enhance perception of 3D layers and “peek” inside the 3D retina. This is a an easy and cost-effective way to visualize the results in 3D instead of just each 2D slice of the volume scan. TODO: cite volview and other related visualization work

5 Design and Implementation

5.1 Language

Primary language for experiments chosen for now is Java due to its more formal nature, better design, memory management. Several convenient frameworks are available for image manipulation and pattern recognition, machine learning in Java as well as easier file management, distributed evaluation, web services, and others the author Mokhov is familiar with. Any Java program can interface a C++ program and vice versa via the Java Native Interface (JNI) Sterns (2001–2005); GCJ Contributors (2007). Most critical and interesting things can be converted to C++ IFF needed at a later date when the experiments are over. These design decisions and implementation are based primarily on Java 6 (1.6.29).

```

// Preprocessing (optional)
1 switch preprocessing method do
2   case Skeletonize/Thin/Fill/Contourize
3     | Optionally binarize per Fabritius et al. (2009);
4     | Use augmented 3D Zhang-Suen transform Zhang and Suen (1984) to cleanse the
5       | image and skeletonize it;
6   endsw
7   case Wavelet
8     | Use 3D dual-tree wavelet transform filter Selesnick et al. (2003);
9   endsw
10  case None
11    | Skip preprocessing;
12  endsw
13 endsw
// Analysis and Detection
14 switch detector method do
15   case ILM
16     | 3D ILM detection per Fabritius et al. (2009);
17   endsw
18   case Canny
19     | Apply the customized Canny edge detection from Yang et al. (2010) on the
      | cleansed image;
20   endsw
21   case Softbody
22     | Expand softbody Song (2007) 3D “bubble” bounded by higher intensity pixels
       | centered at the layers’ middle until the expansion stops;
23     | Contour of the bubble will defined the layer boundaries;
24   endsw
25   case PRISM
26     // May need to learn the models
27     | Build a probabilistic graph layer model;
28     | Treat the problem as a model-checking problem for each pixel in 3D space with
       | PRISM The PRISM Team (2004–2012);
29   endsw
30   case Simulated Annealing
31   endsw
32 endsw
33 Visualize with J3D and OpenGL;
34 ...;
```

Figure 13: Building Our Novel Algorithm

5.2 Architecture

- OCTMARFApp – the main application. The tentatively called application stub for experiments has been created and named OCTMARF. The application's overall structure at the moment of creation was based off MARFCATApp (Mokhov (2010,-, 2011)) and its predecessor WriterIdentApp Mokhov et al. (2009); Mokhov (2008–2012) and others.
- The project has been organized into Java packages for various tasks and it incorporated an old work on pattern thinning, skeletonization and 2D feature extraction based on Zhang-Suen transform Zhang and Suen (1984) that is planned to be extended to 3D per the Ideas section. This code was ported, compiles, and runs; it is found under the `marf.apps.oct.OCTMARF.framework.a2` and its subpackages as of this writing. Already used in preliminary experiments.
- See screenshot of Eclipse on the current project's architectural layout overview in Figure 14.

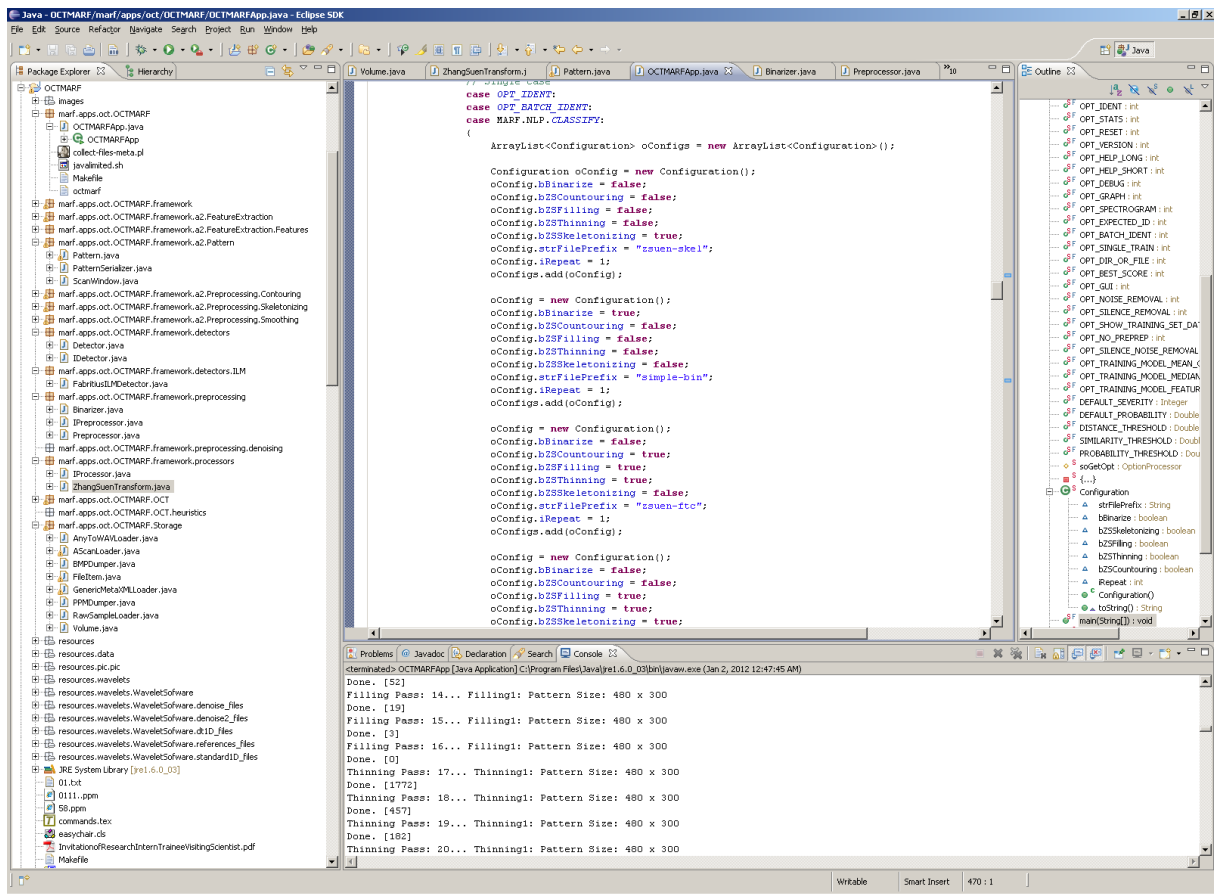


Figure 14: Preliminary Project Layout

5.3 Data Structures

- Volume – a class to contain the 3D OCT volume data.
- consists 3D arrays: `short`, `double`, `String` representing all the slice of a retina scan

- **short** – primarily for basic loading from the .txt data and manipulation
- **double** – for general processing, filtering, etc. as most are floating point numbers and many packages work with that, including MARF.
- **String** – for convenience for debugging and PPM output and printing the values

5.4 Data Management

- **AScanLoader** – a class to load the provided .txt scan data into the internal data structures.
- **PPMDumper** – to dump .ppm image format from the internal data structures
- **BMPDumper** – to dump .bmp image format from the internal data structures (not implemented)
- ...

To preliminary tests of loading, basic manipulation, and dumping are successful, as per Figure 16 and Figure 16. These simply illustrate that the data are loaded and interpreted correctly from the provided data set in Section 3.2.

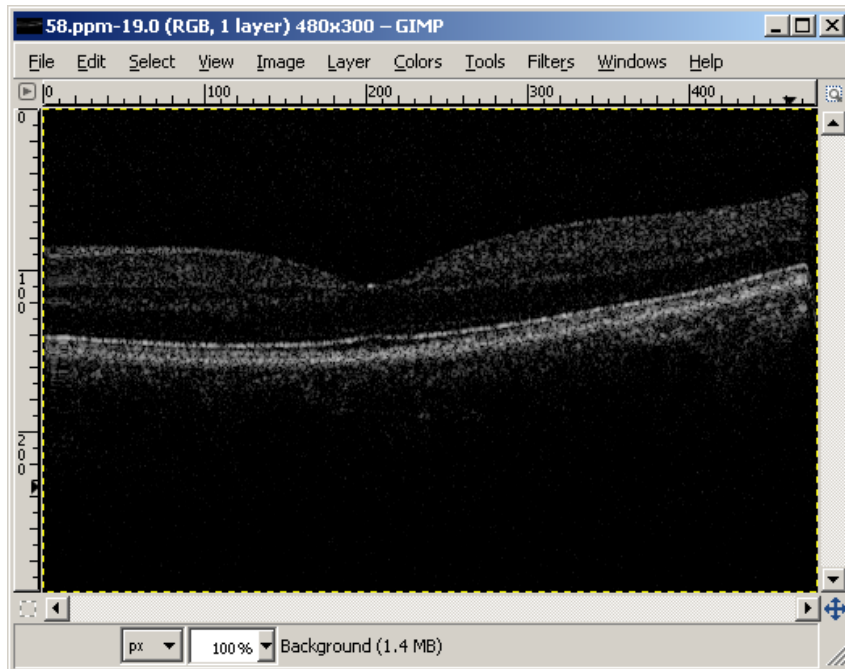


Figure 15: Test of Loading Provided Data in PPM To Match Provided

5.5 APIs

5.5.1 Internal

The internal API at the moment centers around the detector/analyizer/preprocessor frameworks and is invoked by **OCTMARFApp**. Most of them take the **Volume** data structure and do something with it in either 2D or 3D or both. The API provides for both working on the actual **Volume** instance or its copy if desired to preserve the original.

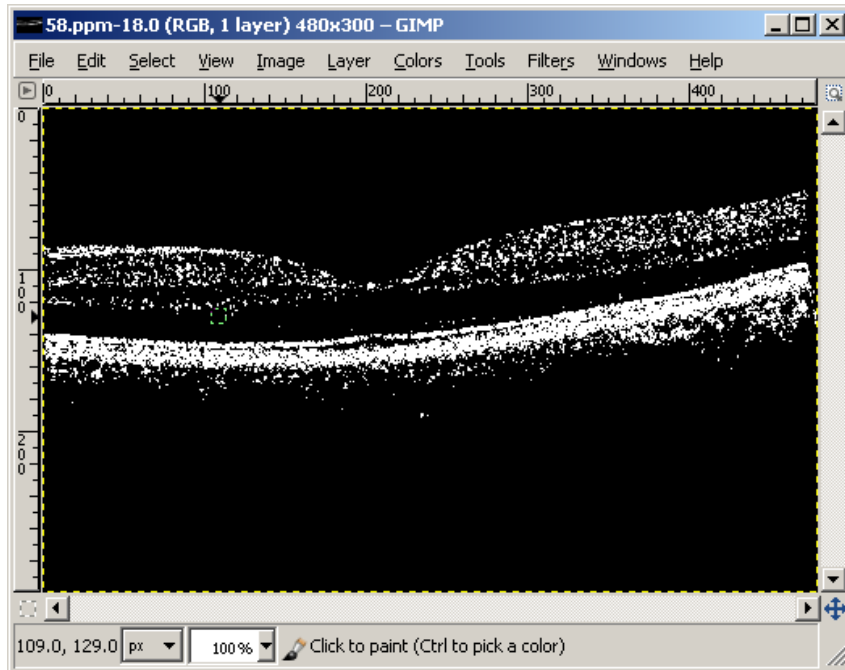


Figure 16: Test of Rudimentary Processing via Threshold

- **IDetector** – specifies the API all boundary detectors should implement
- **Detector** – generic abstract class that concrete classes may inherit from for convenience
- **FabritiusILMDetector** – a specific detector being implemented
- **ZhanSuenTransform** – an example concrete detector and a processor that relies on the implementation of the Zhang and Suen (1984)
- **IPreprocessor** – defines API for all preprocessors (e.g. binarizers, denoisers, or filters or whatever) to use
- **Preprocessor** – a generic class implementing rudimentary API for convenience
- **Binarizer** – a concrete simple preprocessor binarizing images with a set threshold
- **IProcessor** – API for all kinds of analyzers
- **Configuration** – flags and settings for experiment automation
- ...

5.5.2 External

External API has to do with libraries, frameworks, used or planned to be used for evaluation, processing, or connectivity with other platforms and languages.

- MARF The MARF Research and Development Group (2002–2012)
- JAI

- JNI/JNA Sterns (2001–2005)
- GIPSY The GIPSY Research and Development Group (2002–2012)

6 Experiments

Some experiments are in place to test the data processing, the framework’s API operation, and some actual algorithms. That includes loading of the .txt data and its subsequent dump back as an image work (see Figure 15) as well as testing the data structure by rudimentary processing of the loaded data’s pixels by simply discarding values below certain intensity threshold and amplifying the remaining ones to the max as a very basic test (see Figure 16) to ensure the given data understanding is correct via **Binarizer**.

More interesting preliminary results include global 2D (2D at the moment, per slice, but will expand the window to 3D space next) processing that includes in one algorithm some subalgorithms that do preprocessing, skeletonizing, or filling/thinning, and active-contouring of the images from the Zhang-Suen transform. There are many of the options and configurable parameters to try, but already now the outlines of the ILM, IS/OS, RPE can be seen in a very draft debug mode in Figure 19, Figure 20, Figure 17, Figure 18, Figure 21, and Figure 22.

Framework accepts **Configuration** object where multiple configurations with or without preprocessing can be tried on the whole volume.

These can be further refined with parameter tweaking as well as other algorithms (e.g. Canny edge detection, graph search, etc.).

Run-times for the current experiments varied from 29 seconds to 5 minutes depending on the configuration for the whole 3D volume.

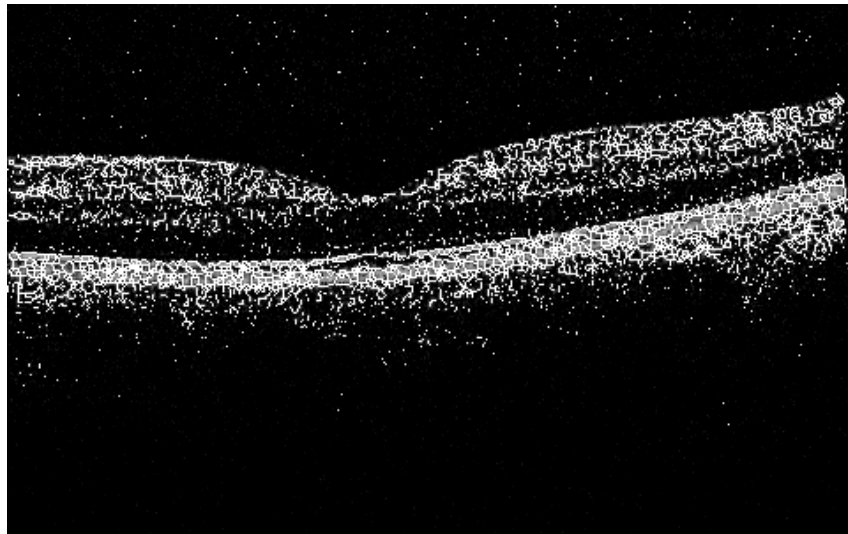


Figure 17: 2D Zhang-Suen Skeletonizing near Fovea

Acknowledgments

Serguei Mokhov is supported in part by the CCSEP scholarship and the Faculty of Engineering and Computer Science (ENCS), Concordia University, Montreal, Canada. Yankui Sun’s research



Figure 18: 2D Zhang-Suen Skeletonizing of Slice 90

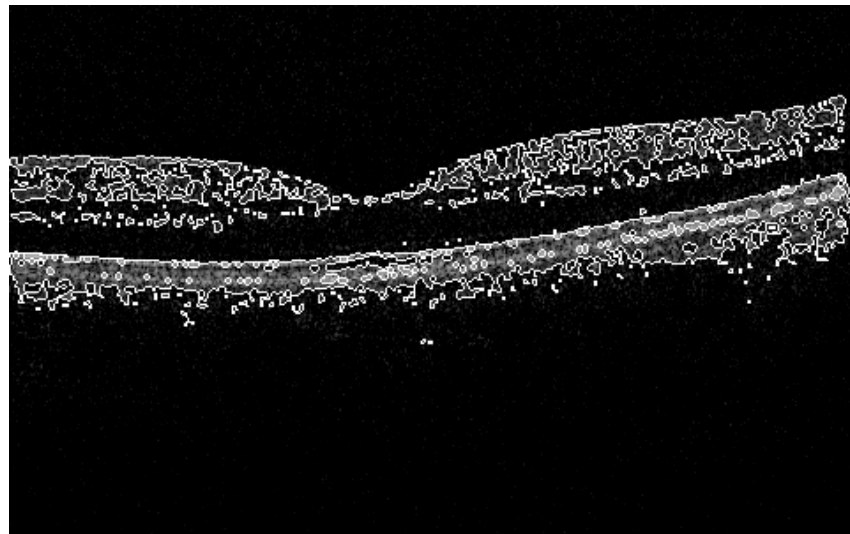


Figure 19: 2D Zhang-Suen Filling-Thinning-Contouring near Fovea

is supported by the National Natural Science Foundation of China no. 60971006.

References

Yazdanpanah Azadeh, Ghassan Hamarneh, and Benjamin R. Smith. Segmentation of intra-retinal layers from optical coherence tomography images using an active contour approach. *IEEE Tran. On Medical Imaging*, 30(2):484–496, February 2011. doi: 10.1109/TMI.2010.2087390.

Maurizio Baroni, S. Diciotti, A. Evangelisti, Pina Fortunato, and Agostino La Torre. Texture classification of retinal layers in optical coherence tomography. In Tomaz Jarm, Peter Kramar, Anze Zupanic, and Ratko Magjarevic, editors, *11th Mediterranean Conference*

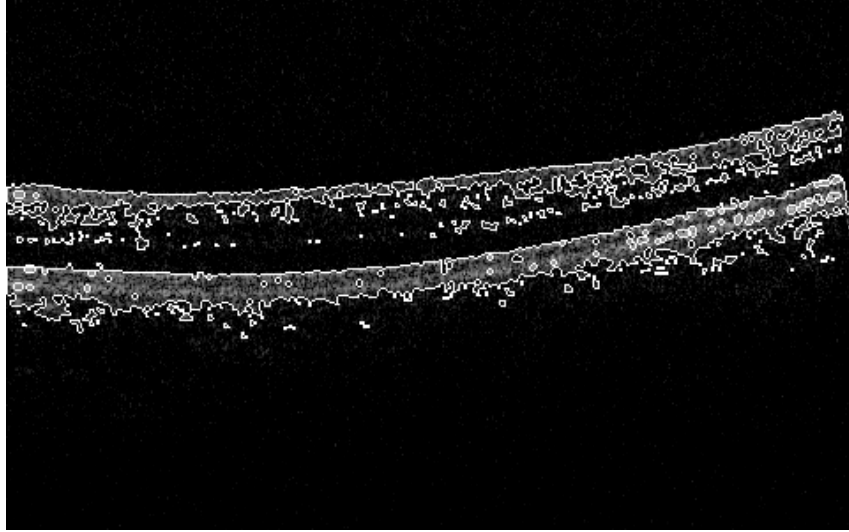


Figure 20: 2D Zhang-Suen Filling-Thinning-Contouring of Slice 90

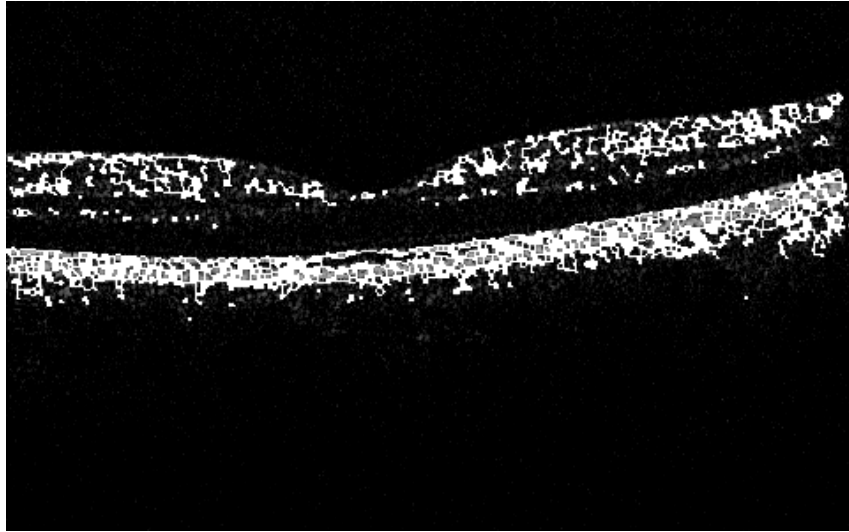


Figure 21: 2D Zhang-Suen Filling-Thinning-Skeletonizing near Fovea

on Medical and Biomedical Engineering and Computing 2007, volume 16 of *IFMBE Proceedings*, pages 847–850. Springer Berlin Heidelberg, 2007a. ISBN 978-3-540-73044-6. doi: 10.1007/978-3-540-73044-6\220.

Maurizio Baroni, Pina Fortunato, and Agostino La Torre. Towards quantitative analysis of retinal features in optical coherence tomography. *Med. Engin. Phys.*, 29:432–441, 2007b.

D. R. Chittajallu, G. Brunner, U. Kurkure, R. P. Yalamanchili, and I.A. Kakadiaris. Fuzzy-Cuts: A knowledge-driven graph-based method for medical image segmentation. In *Proceedings of the IEEE Conference on Computer Vision and Pattern Recognition (CVPR), 2009*, pages 715–722. IEEE, August 2009. ISBN 978-1-4244-3991-1. doi: 10.1109/CVPR.2009.5206623.

Rupsa Datta, S. Aditya, and D. N. Tibrewala. Advancement in OCT and image-processing

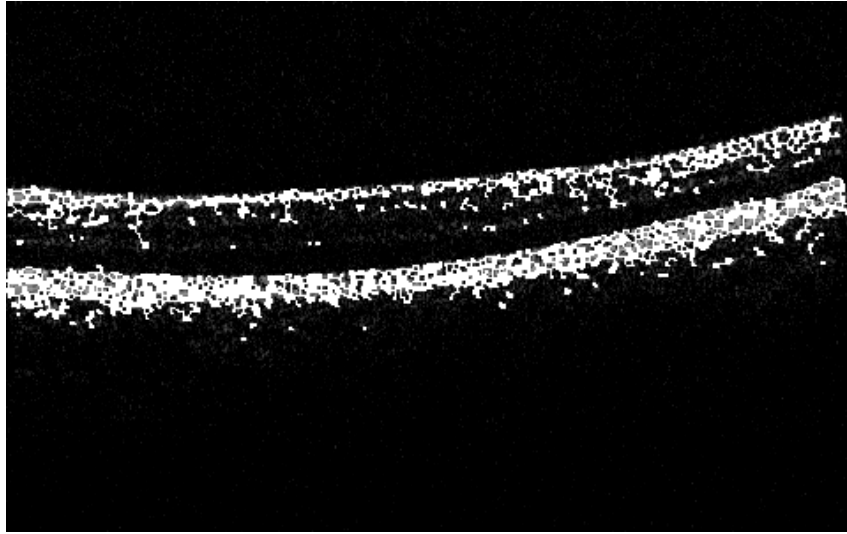


Figure 22: 2D Zhang-Suen Filling-Thinning-Skeletonizing of Slice 90

techniques for automated ophthalmic diagnosis. In *Proceedings of the 2010 IEEE Students' Technology Symposium*, pages 26–32, 2010a.

Rupsa Datta, S. Aditya, and D. N. Tibrewala. Advancement in OCT and image-processing techniques for automated ophthalmic diagnosis. In *Proceedings of the 2010 IEEE Students' Technology Symposium*, pages 26–33. IEEE, April 2010b. ISBN 978-1-4244-5974-2.

Delia Cabrera Debuc, Harry M. Salinas, and Sudarshan Ranganathan. Improving image segmentation performance and quantitative analysis via a computer-aided grading methodology for optical coherence tomography retinal image analysis. *Journal of Biomedical Optics*, 15(4):484–496, 2010.

Wolfgang Drexler and James G. Fujimoto. State-of-the-art retinal optical coherence tomography. *Progress in Retinal and Eye Research*, 27:45–88, 2008.

Tapio Fabritius, Shuichi Makita, Masahiro Miura, Risto Myllylä, and Yoshiaki Yasuno. Automated segmentation of the macula by optical coherence tomography. *Optics Express*, 17(18), August 2009. doi: 10.1364/OE.17.015659. 15659.

Delia Cabrera Fernández, Harry M. Salinas, and Carmen A. Puliafito. Automated detection of retinal layer structures on optical coherence tomography images. *Optics Express*, 13(25):200–216, 2005.

Alfred R. Fuller, Robert J. Zawadzki, Stacey Choi, David F. Wiley, John S. Werner, and Bernd Hamann. Segmentation of three-dimensional retinal image data. *IEEE Transactions on Visualization and Computer Graphics*, 13(6):1719–1726, 2007. doi: 10.1109/TVCG.2007.70590.

Mona Kathryn Garvin, Michael David Abramoff, R. Kardon, S. R. Russell, Xiaodong Wu, and M. Sonka. Intraretinal layer segmentation of macular optical coherence tomography images using optimal 3-D graph search. *IEEE Tran. On Medical Imaging*, 10(10):1495–1505, 2008.

Mona Kathryn Garvin, Michael David Abramoff, and Xiaodong Wu. Automated 3-D intraretinal layer segmentation of macular spectral-domain optical coherence tomography images. *IEEE Tran. On Medical Imaging*, 28(9):1436–1447, September 2009.

GCJ Contributors. The Compiled Native Interface (CNI). [online], 2007. <http://gcc.gnu.org/onlinedocs/gcj/About-CNI.html>.

Itebeddine Ghorbel, Florence Rossant, Isabelle Bloch, Sarah Tick, and Michel Paques. Automated segmentation of macular layers in OCT images and quantitative evaluation of performances. *Pattern Recognition*, 44(8):1590–1603, 2011. ISSN 0031-3203. doi: 10.1016/j.patcog.2011.01.012. Online at <http://www.sciencedirect.com/science/article/pii/S0031320311000380>.

Shivani Haridas. Generation of 2-D digital filters with variable magnitude characteristics starting from a particular type of 2-variable continued fraction expansion. Master’s thesis, Department of Electrical and Computer Engineering, Concordia University, Montreal, Canada, July 2006.

D. Huang, E. A. Swanson, C. P. Lin, et al. Optical coherence tomography. *Science*, 254(5035): 1178–1181, 1991.

Hiroshi Ishikawa, Daniel M. Stein, Gadi Wollstein, Siobahn Beaton, James G. Fujimoto, and Joel S. Schuman. Macular segmentation with optical coherence tomography. *Investigative Ophthalmol. Visual Scie.*, 46:2012–2017, 2005.

V. Kajic et al. Robust segmentation of intraretinal layers in the normal human fovea using a novel statistical model based on texture and shape analysis. *Optics Express*, 18(14), 2010.

Manesh Kokare, P. K. Biswas, and B. N. Chatterji. Texture image retrieval using new rotated complex wavelet filters. *IEEE Transaction on Systems, Man, and Cybernetics-Part B: Cybernetics*, 6(35):1168–1178, 2005.

Manesh Kokare, P. K. Biswas, and B. N. Chatterji. Rotation-invariant texture image retrieval using rotated complex wavelet filters. *IEEE Transaction on Systems, Man, and Cybernetics-Part B: Cybernetics*, 6(36):1273–1282, 2006.

Dara Koozekanani, Kim Boyer, and Cynthia Roberts. Retinal thickness measurements from optical coherence tomography using a markov boundary model. *IEEE Transactions on Medical Imaging*, 20(9):900–916, 2001.

Zongqing Lu, Qingmin Liao, and Fan Yang. A variational approach to automatic segmentation of RNFL on OCT data sets of the retina. In *16th IEEE International Conference on Image Processing*, volume 1–6, pages 3309–3312, November 2009.

Serguei A. Mokhov. WriterIdentApp – Writer Identification Application. Unpublished, 2008–2012.

Serguei A. Mokhov. The use of machine learning with signal- and NLP processing of source code to fingerprint, detect, and classify vulnerabilities and weaknesses with MARFCAT. [online], October 2010. Online at <http://arxiv.org/abs/1010.2511>.

Serguei A. Mokhov. MARFCAT – MARF-based Code Analysis Tool. Published electronically within the MARF project, <http://sourceforge.net/projects/marf/files/Applications/MARFCAT/>, 2010–2012. Last viewed April 2012.

Serguei A. Mokhov. The use of machine learning with signal- and NLP processing of source code to fingerprint, detect, and classify vulnerabilities and weaknesses with MAR-FCAT. Technical Report NIST SP 500-283, NIST, October 2011. Report: http://www.nist.gov/manuscript-publication-search.cfm?pub_id=909407, online e-print at <http://arxiv.org/abs/1010.2511>.

Serguei A. Mokhov, Marc-André Laverdière, Nader Hatami, and Ali Benssam. Cryptolysis – a framework for automated cryptanalysis of classical ciphers. SourceForge.net, 2005–2012a. <http://ciisesec cvs.sourceforge.net/ciisesec/crypto/>, last viewed April 2008.

Serguei A. Mokhov, Marc-André Laverdière, Nader Hatami, and Ali Benssam. Cryptolysis v.0.0.1 – a framework for automated cryptanalysis of classical ciphers. [online], 2005–2012b. Project report; <http://arxiv.org/abs/1101.1075>.

Serguei A. Mokhov, Miao Song, and Ching Y. Suen. Writer identification using inexpensive signal processing techniques. In Tarek Sobh and Khaled Elleithy, editors, *Innovations in Computing Sciences and Software Engineering; Proceedings of CISSE'09*, pages 437–441. Springer, December 2009. doi: 10.1007/978-90-481-9112-3_74. ISBN: 978-90-481-9111-6, online at: <http://arxiv.org/abs/0912.5502>.

M. Mujat, R. C. Chan, B. Cense, B. H. Park, C. Joo, T. Akkin, T. C. Chen, and J. F. de Boer. Retinal nerve fiber layer thickness map determined from optical coherence tomography images. *Opt. Express*, 13:9480–9491, 2005.

OpenGL Architecture Review Board. OpenGL. [online], 1998–2012. <http://www.opengl.org>.

Ivan Selesnick, Shihua Cai, Keyong Li, Levent Sendur, and A. Farris Abdehnour. MATLAB implementation of wavelet transforms. Technical report, Electrical Engineering, Polytechnic University, Brooklyn, NY, 2003. Online at <http://taco.poly.edu/WaveletSoftware/>.

Miao Song. Dynamic deformation of uniform elastic two-layer objects. Master's thesis, Department of Computer Science and Software Engineering, Concordia University, Montreal, Canada, August 2007. ISBN: 978-0-4943-4780-5, <http://arxiv.org/abs/0907.4364>.

Beth Sterns. The Java Native Interface (JNI). [online], 2001–2005. <http://java.sun.com/developer/onlineTraining/Programming/JDCBook/jni.html>.

Yankui Sun and Ming Lei. Method for optical coherence tomography image classification using local features and earth mover's distance. *Journal of Biomedical Optics*, 14(5), 2009. 054037.

Yankui Sun and Ming Lei. Automated thickness measurements of nacre from optical coherence tomography using polar transform and probability density projection. In *Proceedings of the 18th International Symposium on Intelligent Signal Processing and Communications Systems*, pages 505–508, 2010.

Yankui Sun and Tian Zhang. A 3D segmentation method for retinal optical coherence tomography volume data. [online], 2012. Submitted for publication to EMBC2012. online at <http://arxiv.org/abs/1204.6385>.

M. Szkulmowski, M. Wojtkowski, B. Sikorski, T. Bajraszewski, V. J. Srinivasan, A. Szkulmowska, J. J. Kaluzny, James G. Fujimoto, and A. Kowalczyk. Analysis of posterior retinal layers in spectral optical coherence tomography images of the normal retina and retinal pathologies. *J. Biomed. Opt.*, 12, 2007.

The GIPSY Research and Development Group. The General Intensional Programming System (GIPSY) project. Department of Computer Science and Software Engineering, Concordia University, Montreal, Canada, 2002–2012. <http://newton.cs.concordia.ca/~gipsy/>, last viewed April 2012.

The MARF Research and Development Group. The Modular Audio Recognition Framework and its Applications. [online], 2002–2012. <http://marf.sf.net> and <http://arxiv.org/abs/0905.1235>, last viewed April 2012.

The PRISM Team. PRISM: a probabilistic model checker. [online], 2004–2012. <http://www.prismmodelchecker.org/>, last viewed June 2010.

J. Weickert, B. H. Romeny, and M. Viergever. Efficient and reliable schemes for nonlinear diffusion filtering. *IEEE Transactions on Image Processing*, 7(3):398–410, 1998.

Qi Yang, Charles A. Reisman, Zhenguo Wang, Yasufumi Fukuma, Masanori Hangai, Nagahisa Yoshimura, Atsuo Tomidokoro, Makoto Araie, Ali S. Raza, Donald C. Hood, and Kinpui Chan. Automated layer segmentation of macular OCT images using dual-scale gradient information. *Optics Express*, 18(20):21293–21307, September 2010. doi: 10.1364/OE.18.021293.

Robert J. Zawadzki, Alfred R. Fuller, David F. Wiley, et al. Adaptation of a support vector machine algorithm for segmentation and visualization of retinal structures in volumetric optical coherence tomography data sets. *Journal of Biomedical Optics*, 12(4), 2007.

T. Y. Zhang and Ching Y. Suen. A fast parallel algorithm for thinning digital patterns. *Communications of the ACM*, 27(3):236–239, March 1984. ISSN 0001-0782. doi: 10.1145/357994.358023.

A Proof-of-Concept Code Excerpts

A.1 AScanLoader

```
package marf.apps.oct.OCTMARF.Storage;

import java.io.BufferedReader;
import java.io.File;
import java.io.FileReader;
import java.io.IOException;

import marf.apps.oct.OCTMARF.framework.processors.ZhangSuenTransform;
import marf.util.Arrays;

/**
 * Loads and parses A-scans from .txt files into internal data structures.
 *
 * @author Serguei Mokhov
 * @since 0.0.1, October 30, 2011
 * @version $Id: AScanLoader.java,v 1.8 2012/01/02 08:06:32 mokhov Exp $
 */
public class AScanLoader
{
    /**
     * 3D image volume storage.
     */
    protected Volume oVolume = new Volume();

    /**

```

```

 * Current slice to process.
 * Usually during loading.
 */
protected int iScanSlice = 0;

/**
 * Empty loader.
 */
public AScanLoader()
{
}

/***
 * Should the scan fail to load.
 * @param pstrSampleFilename
 * @throws IOException
 * @see {@link #load(String)}
 */
public AScanLoader(String pstrSampleFilename)
throws IOException
{
    load(pstrSampleFilename);
}

/***
 * Loads the current specified slice.
 * @param pstrSampleFilename
 * @throws IOException
 */
public void load(String pstrSampleFilename)
throws IOException
{
    BufferedReader oBFR = new BufferedReader(new FileReader(pstrSampleFilename));
    String strDataLine = oBFR.readLine();

    int iAScanLine = 0;

    while(strDataLine != null)
    {
        //System.out.println("Data line: [" + strDataLine + "]");

        String[] astrPixels = strDataLine.split(" ");
        //System.out.println("Data line element count: [" + astrPixels.length + "]");

        //this.astr3DScan[this.iScanSlice][iAScanLine] = astrPixels;
        //Arrays.copy(this.as3DScan[this.iScanSlice][iAScanLine], astrPixels);
        //Arrays.copy(this.ad3DScan[this.iScanSlice][iAScanLine], this.as3DScan[this.iScanSlice][iAScanLine]);

        this.oVolume.astr3DScan[this.iScanSlice][iAScanLine] = astrPixels;
        Arrays.copy(this.oVolume.as3DScan[this.iScanSlice][iAScanLine], astrPixels);
        Arrays.copy(this.oVolume.ad3DScan[this.iScanSlice][iAScanLine], this.oVolume.as3DScan[this.iScanSlice][iAScanLine]);

        iAScanLine++;
        strDataLine = oBFR.readLine();
        //strDataLine = null;
    }

    oBFR.close();

    // Move to the next slice for (potential) loading
    this.iScanSlice++;
}

/***
 * @return
 */
public short[][][] getShort3DScan()
{
}

```

```

        return this.oVolume.as3DScan;
    }

    /**
     * @return
     */
    public double[][][] getDouble3DScan()
    {
        return this.oVolume.ad3DScan;
    }

    /**
     * @return
     */
    public String[][][] getString3DScan()
    {
        return this.oVolume.astr3DScan;
    }

    public Volume getVolume()
    {
        return this.oVolume;
    }

    public int sizeInSlices()
    {
        return this.iScanSlice + 1;
    }
}

// EOF

```

A.2 Volume

```

package marf.apps.oct.OCTMARF.Storage;

import java.io.Serializable;

/**
 * TODO: document.
 *
 * $Id: Volume.java,v 1.1 2011/12/18 07:17:34 mokhov Exp $
 *
 * @author serguei
 * @since
 */
public class Volume
implements Serializable, Cloneable
{
    /**
     *
     */
    private static final long serialVersionUID = -6995648761632634728L;

    /**
     * A-scan's line.
     */
    public static final int DEFAULT_SCAN_HEIGHT = 300;

    /**
     * Normal scan dimension.
     */
    public static final int DEFAULT_SCAN_WIDTH = 480;

    /**
     * Number of scan slices.
     */
}

```

```
/*
public static final int DEFAULT_SCAN_DEPTH = 100;

protected short[][][] as3DScan = new short[DEFAULT_SCAN_DEPTH][DEFAULT_SCAN_WIDTH][DEFAULT_SCAN_HEIGHT];
protected double[][][] ad3DScan = new double[DEFAULT_SCAN_DEPTH][DEFAULT_SCAN_WIDTH][DEFAULT_SCAN_HEIGHT];
protected String[][][] astr3DScan = new String[DEFAULT_SCAN_DEPTH][DEFAULT_SCAN_WIDTH][DEFAULT_SCAN_HEIGHT];

private boolean bEmpty = true;

public Volume()
{
    super();
}

/**
 * @return the as3DScan
 */
public short[][][] getShort3DScan()
{
    return as3DScan;
}

/**
 * @param as3dScan the as3DScan to set
 */
public void setShort3DScan(short[][][] as3dScan) {
    as3DScan = as3dScan;
}

/**
 * @return the ad3DScan
 */
public double[][][] getDouble3DScan() {
    return ad3DScan;
}

/**
 * @param ad3dScan the ad3DScan to set
 */
public void setDouble3DScan(double[][][] ad3dScan) {
    ad3DScan = ad3dScan;
}

/**
 * @return the astr3DScan
 */
public String[][][] getString3DScan() {
    return astr3DScan;
}

/**
 * @param astr3dScan the astr3DScan to set
 */
public void setString3DScan(String[][][] astr3dScan) {
    astr3DScan = astr3dScan;
}

public boolean isEmpty()
{
    return this.bEmpty;
}

/* (non-Javadoc)
 * @see java.lang.Object#clone()
 */
@Override
public Object clone()
```

```

//throws CloneNotSupportedException
{
    Volume oCopy = null;

    try
    {
        oCopy = (Volume)super.clone();

        if(this.ad3DScan != null)
        {
            oCopy.ad3DScan = this.ad3DScan.clone();
        }

        if(this.as3DScan != null)
        {
            oCopy.as3DScan = this.as3DScan.clone();
        }

        if(this.astr3DScan != null)
        {
            oCopy.astr3DScan = this.astr3DScan.clone();
        }
    }
    catch(CloneNotSupportedException e)
    {
        System.err.println("Failed to clone volume.");
        e.printStackTrace(System.err);
    }

    return oCopy;
}

/* (non-Javadoc)
 * @see java.lang.Object#finalize()
 */
@Override
protected void finalize()
throws Throwable
{
    this.ad3DScan = null;
    this.as3DScan = null;
    this.astr3DScan = null;
    super.finalize();
}

/* (non-Javadoc)
 * @see java.lang.Object#toString()
 */
@Override
public String toString()
{
    return "}: empty: " + this.bEmpty;
}
}

// EOF

```

A.3 OCTMARFApp

```

package marf.apps.oct.OCTMARF;

import java.io.File;
import java.util.ArrayList;

import marf.MARF;
import marf.Classification.Distance.HammingDistance;
import marf.Storage.ModuleParams;

```

```
import marf.Storage.TrainingSet;
import marf.apps.oct.OCTMARF.Storage.AScanLoader;
import marf.apps.oct.OCTMARF.Storage.AnyToWAVLoader;
import marf.apps.oct.OCTMARF.Storage.PPMDumper;
import marf.apps.oct.OCTMARF.Storage.RawSampleLoader;
import marf.apps.oct.OCTMARF.framework.preprocessing.Binarizer;
import marf.apps.oct.OCTMARF.framework.processors.ZhangSuenTransform;
import marf.util.Debug;
import marf.util.MARFException;
import marf.util.NotImplementedException;
import marf.util.OptionProcessor;

<**
 * <p>
 * A an OCT image processing testbed platform for various algorithms.
 * </p>
 *
 * @author Serguei Mokhov
 *
 * @version $Id: OCTMARFApp.java,v 1.6 2012/01/02 08:06:32 mokhov Exp $
 * @since October 2011
 */
public class OCTMARFApp
{
    /*
     * -----
     * Apps. Versioning -----
     */

    /**
     * Current major version of the application.
     */
    public static final int MAJOR_VERSION = 0;

    /**
     * Current minor version of the application.
     */
    public static final int MINOR_VERSION = 0;

    /**
     * Current revision of the application.
     */
    public static final int REVISION = 1;

    /*
     * -----
     * Defaults
     * -----
     */

    /**
     * Default file name extension for sample files; case-insensitive.
     */
    public static final String DEFAULT_SAMPLE_FILE_EXTENSION = "txt";

    /*
     * -----
     * Major and Misc Options Enumeration
     * -----
     */

    /**
     * Numeric equivalent of the option <code>--train</code>.
     */
    public static final int OPT_TRAIN = 0;

    /**
     * Numeric equivalent of the option <code>--ident</code>.
     */
```

```

/*
public static final int OPT_IDENT = 1;

/**
 * Numeric equivalent of the option <code>--stats</code>.
 */
public static final int OPT_STATS = 2;

/**
 * Numeric equivalent of the option <code>--reset</code>.
 */
public static final int OPT_RESET = 3;

/**
 * Numeric equivalent of the option <code>--version</code>.
 */
public static final int OPT_VERSION = 4;

/**
 * Numeric equivalent of the option <code>--help</code>.
 */
public static final int OPT_HELP_LONG = 5;

/**
 * Numeric equivalent of the option <code>-h</code>.
 */
public static final int OPT_HELP_SHORT = 6;

/**
 * Numeric equivalent of the option <code>-debug</code>.
 */
public static final int OPT_DEBUG = 7;

/**
 * Numeric equivalent of the option <code>-graph</code>.
 */
public static final int OPT_GRAPH = 8;

/**
 * Numeric equivalent of the option <code>-spectrogram</code>.
 */
public static final int OPT_SPECTROGRAM = 9;

/**
 * Numeric equivalent of the option <code>&lt;writer ID&gt;</code>.
 */
public static final int OPT_EXPECTED_ID = 10;

/**
 * Numeric equivalent of the option <code>--batch-ident</code>.
 */
public static final int OPT_BATCH_IDENT = 11;

/**
 * Numeric equivalent of the option <code>--single-train</code>.
 */
public static final int OPT_SINGLE_TRAIN = 12;

/**
 * Numeric equivalent of the option
 * <code>&lt;sample-file-or-directory-name&gt;</code>.
 */
public static final int OPT_DIR_OR_FILE = 13;

/**
 * Numeric equivalent of the option <code>--best-score</code>.
 */
public static final int OPT_BEST_SCORE = 14;

```

```

/**
 * Numeric equivalent of the option <code>--gui</code> to have a GUI.
 */
public static final int OPT_GUI = 15;

/**
 * Numeric equivalent of the option <code>-noise</code> to enable noise
 * removal.
 */
public static final int OPT_NOISE_REMOVAL = 16;

/**
 * Numeric equivalent of the option <code>-silence</code> to enable silence
 * removal.
 */
public static final int OPT_SILENCE_REMOVAL = 17;

/**
 * Numeric equivalent of the option <code>--show-training-set</code> to
 * display text representation of a training set file.
 */
public static final int OPT_SHOW_TRAINING_SET_DATA = 18;

public static final int OPT_NO_PREPREP = 20;

public static final int OPT_SILENCE_NOISE_REMOVAL = 27;

public static final int OPT_TRAINING_MODEL_MEAN_CLUSTER = 29;
public static final int OPT_TRAINING_MODEL_MEDIAN_CLUSTER = 30;
public static final int OPT_TRAINING_MODEL_FEATURE_SET = 31;

/*
 * Some defaults
 */

public static final Integer DEFAULT_SEVERITY = 2;
public static final Double DEFAULT_PROBABILITY = 0.0;

public static final Double DISTANCE_THRESHOLD = 0.1;
public static final Double SIMILARITY_THRESHOLD = 0.001;
public static final Double PROBABILITY_THRESHOLD = 0.9;

/*
 * -----
 * State Data Structures
 * -----
 */

/**
 * Instance of the option processing utility.
 */
protected static OptionProcessor soGetOpt = new OptionProcessor();

/*
 * ----- Static State Init -----
 */

static
{
    // Main options
    soGetOpt.addValidOption(OPT_TRAIN, "--train");
    soGetOpt.addValidOption(OPT_SINGLE_TRAIN, "--single-train");
    soGetOpt.addValidOption(OPT_IDENT, "--ident");
    soGetOpt.addValidOption(OPT_BATCH_IDENT, "--batch-ident");
    soGetOpt.addValidOption(OPT_STATS, "--stats");
    soGetOpt.addValidOption(OPT_BEST_SCORE, "--best-score");
    soGetOpt.addValidOption(OPT_SHOW_TRAINING_SET_DATA, "--show-training-set");
}

```

```

soGetOpt.addValidOption(OPT_VERSION, "--version");
soGetOpt.addValidOption(OPT_RESET, "--reset");
soGetOpt.addValidOption(OPT_HELP_LONG, "--help");
soGetOpt.addValidOption(OPT_HELP_SHORT, "-h");
soGetOpt.addValidOption(OPT_DEBUG, "--debug");

// Sample Loading
soGetOpt.addValidOption(MARF.TEXT, "-text");

// Preprocessing
soGetOpt.addValidOption(OPT_NOISE_REMOVAL, "-noise");
soGetOpt.addValidOption(OPT_SILENCE_REMOVAL, "-silence");
soGetOpt.addValidOption(OPT_SILENCE_NOISE_REMOVAL, "-silence-noise");

soGetOpt.addValidOption(MARF.DUMMY, "-norm");
soGetOpt.addValidOption(MARF.HIGH_FREQUENCY_BOOST_FFT_FILTER, "-boost");
soGetOpt.addValidOption(MARF.HIGH_PASS_FFT_FILTER, "-high");
soGetOpt.addValidOption(MARF.LOW_PASS_FFT_FILTER, "-low");
soGetOpt.addValidOption(MARF.BANDPASS_FFT_FILTER, "-band");
soGetOpt.addValidOption(MARF.BAND_STOP_FFT_FILTER, "-bandstop");
soGetOpt.addValidOption(MARF.HIGH_PASS_BOOST_FILTER, "-highpassboost");
soGetOpt.addValidOption(MARF.RAW, "-raw");
soGetOpt.addValidOption(MARF.ENDPOINT, "-endp");
soGetOpt.addValidOption(MARF.HIGH_PASS_CFE_FILTER, "-highcfe");
soGetOpt.addValidOption(MARF.LOW_PASS_CFE_FILTER, "-lowcfe");
soGetOpt.addValidOption(MARF.BAND_PASS_CFE_FILTER, "-bandcfe");
soGetOpt.addValidOption(MARF.BAND_STOP_CFE_FILTER, "-bandstopcfe");

// Wavelets
soGetOpt.addValidOption(MARF.SEPARABLE_DWT_FILTER, "-sdwt");
soGetOpt.addValidOption(MARF.DUAL_DTREE_DWT_FILTER, "-dualtree");
soGetOpt.addValidOption(MARF.DYADIC_DWT_FILTER, "-dyadic");

// Feature extraction
soGetOpt.addValidOption(MARF.FFT, "-fft");
soGetOpt.addValidOption(MARF.LPC, "-lpc");
soGetOpt.addValidOption(MARF.RANDOM_FEATURE_EXTRACTION, "-randfe");
soGetOpt.addValidOption(MARF.MIN_MAX_AMPLITUDES, "-minmax");
soGetOpt.addValidOption(MARF.FEATURE_EXTRACTION_AGGREGATOR, "-aggr");
soGetOpt.addValidOption(MARF.FO, "-f0");
soGetOpt.addValidOption(MARF.SEGMENTATION, "-segm");
soGetOpt.addValidOption(MARF.CEPSTRAL, "-cepstral");

// Classification
soGetOpt.addValidOption(MARF.NEURAL_NETWORK, "-nn");
soGetOpt.addValidOption(MARF.EUCLIDEAN_DISTANCE, "-eucl");
soGetOpt.addValidOption(MARF.CHEBYSHEV_DISTANCE, "-cheb");
soGetOpt.addValidOption(MARF.MINKOWSKI_DISTANCE, "-mink");
soGetOpt.addValidOption(MARF.MAHALANOBIS_DISTANCE, "-mah");
soGetOpt.addValidOption(MARF.RANDOM_CLASSIFICATION, "-randc1");
soGetOpt.addValidOption(MARF.DIFF_DISTANCE, "-diff");
soGetOpt.addValidOption(MARF.ZIPFS_LAW, "-zipf");
soGetOpt.addValidOption(MARF.MARKOV, "-markov");
soGetOpt.addValidOption(MARF.HAMMING_DISTANCE, "-hamming");
soGetOpt.addValidOption(MARF.COSINE_SIMILARITY_MEASURE, "-cos");

// Graphical
soGetOpt.addValidOption(OPT_SPECTROGRAM, "-spectrogram");
soGetOpt.addValidOption(OPT_GRAPH, "-graph");
soGetOpt.addValidOption(OPT_GUI, "--gui");

// NLP
soGetOpt.addValidOption(MARF.EStatisticalEstimatorsMLE, "-mle");
soGetOpt.addValidOption(MARF.EStatisticalEstimatorsADD_ONE, "-add-one");
soGetOpt.addValidOption(MARF.EStatisticalEstimatorsADD_DELTA, "-add-delta");
soGetOpt.addValidOption(MARF.EStatisticalEstimatorsELE, "-ele");
soGetOpt.addValidOption(MARF.EStatisticalEstimatorsWITTEN_BELL, "-witten-bell");

```

```

soGetOpt.addValidOption(MARF.EStatisticalEstimators.GOOD_TURING, "-good-turing");
soGetOpt.addValidOption(MARF.EStatisticalEstimators.SLI, "-sli");
soGetOpt.addValidOption(MARF.EStatisticalEstimators.GLI, "-gli");
soGetOpt.addValidOption(MARF.EStatisticalEstimators.KATZ_BACKOFF, "-backoff");

soGetOpt.addValidOption(MARF.NLP.STEMMING, "-stemming");

soGetOpt.addValidOption(MARF.NLP.CHARACTER_MODE, "-char");
soGetOpt.addValidOption(MARF.NLP.WORD_MODE, "-word");

soGetOpt.addValidOption(MARF.NLP.CASE_SENSITIVE, "-case");
soGetOpt.addValidOption(MARF.NLPPARSE_NUMBERS, "-num");
soGetOpt.addValidOption(MARF.NLPPARSE_QUOTED_STRINGS, "-quote");
soGetOpt.addValidOption(MARF.NLPPARSE_ENDS_OF_SENTENCE, "-eos");
soGetOpt.addValidOption(MARF.NLPRAW_ZIPFS_LAW_DUMP, "-nolog");

soGetOpt.addValidOption(MARF.ENgramModels.UNIGRAM, "-unigram");
soGetOpt.addValidOption(MARF.ENgramModels.BIGRAM, "-bigram");
soGetOpt.addValidOption(MARF.ENgramModels.TRIGRAM, "-trigram");

soGetOpt.addValidOption(MARF.NLP.TRAIN, "--train-nlp");
soGetOpt.addValidOption(MARF.NLP.CLASSIFY, "--ident-nlp");

soGetOpt.addValidOption(MARF.NLP.ZIPFS_LAW_CHEAT, "--cheat");

soGetOpt.addValidOption(MARF.NLP.INTERACTIVE, "-interactive");

soGetOpt.addValidOption(OPT_NO_PREPREG, "-noprepreg");
}

public static class Configuration
{
    String strFilePrefix = "";
    boolean bBinarize = false;
    boolean bZSSkeletonizing = false;
    boolean bZSFilling = false;
    boolean bZSThinning = false;
    boolean bZSCountouring = false;

    int iRepeat = 1;

    public Configuration()
    {

    }

    public String toString()
    {
        return strFilePrefix + ":" + bBinarize + ":" + bZSSkeletonizing + ":" + bZSFilling + ":" + bZSThinning + ":" + bZSCountouring;
    }
}

/**
 * Main body.
 *
 * @param argv command-line arguments
 */
public static final void main(String[] argv)
{
    try
    {
        // Since some new API is always introduced...
        validateVersions();

        // Parse extra arguments
        int iValidOptions = soGetOpt.parse(argv);

        // Turn on command-line supplied debugging
    }
}

```

```

Debug.enableDebug(soGetOpt.isActiveOption(OPT_DEBUG));
Debug.debug("Option set parsed: " + soGetOpt);

if(iValidOptions == 0)
{
    throw new Exception("No valid options found: " + soGetOpt);
}

switch(soGetOpt.getInvalidOptions().size())
{
    case 0:
    {
        break;
    }

    /*
     * In the case of a single invalid option always assume it
     * is either a filename or a directory name for the --ident
     * or --train options.
     */
    case 1:
    {
        soGetOpt.addActiveOption(OPT_DIR_OR_FILE, soGetOpt.getInvalidOptions().firstElement().toString());
        soGetOpt.getInvalidOptions().clear();
        break;
    }

    default:
    {
        throw new Exception("Unrecognized options found: " + soGetOpt.getInvalidOptions());
    }
}

setDefaultConfig();
setCustomConfig();

// Set misc configuration
MARF.setDumpSpectrogram(soGetOpt.isActiveOption(OPT_SPECTROGRAM));
MARF.setDumpWaveGraph(soGetOpt.isActiveOption(OPT_GRAPH));

Debug.debug("Option set: " + soGetOpt);

if(soGetOpt.isActiveOption(MARF.TEXT))
{
    MARF.setSampleFormat(MARF.TEXT);
    MARF.setSampleLoaderPluginClass(AnyToWAVLoader.class.getName());
    System.out.println("Using text loader");
}
else if(soGetOpt.isActiveOption(MARF.TEXT + 2))
{
    MARF.setSampleFormat(MARF.CUSTOM);
    // XXX:
    MARF.setSampleLoaderPluginClass(RawSampleLoader.class.getName());
}

int iMainOption = soGetOpt.getOption(argv[0]);

switch(iMainOption)
{
    /*
     * -----
     * Identification
     * -----
     */

    // Single case
    case OPT_IDENT:
    case OPT_BATCH_IDENT:

```

```
case MARF.NLP.CLASSIFY:  
{  
    ArrayList<Configuration> oConfigs = new ArrayList<Configuration>();  
  
    Configuration oConfig = new Configuration();  
    oConfig.bBinarize = false;  
    oConfig.bZSCountouring = false;  
    oConfig.bZSFilling = false;  
    oConfig.bZSThinning = false;  
    oConfig.bZSSkeletonizing = true;  
    oConfig.strFilePrefix = "zsuen-skel";  
    oConfig.iRepeat = 1;  
    oConfigs.add(oConfig);  
  
    oConfig = new Configuration();  
    oConfig.bBinarize = true;  
    oConfig.bZSCountouring = false;  
    oConfig.bZSFilling = false;  
    oConfig.bZSThinning = false;  
    oConfig.bZSSkeletonizing = false;  
    oConfig.strFilePrefix = "simple-bin";  
    oConfig.iRepeat = 1;  
    oConfigs.add(oConfig);  
  
    oConfig = new Configuration();  
    oConfig.bBinarize = false;  
    oConfig.bZSCountouring = true;  
    oConfig.bZSFilling = true;  
    oConfig.bZSThinning = true;  
    oConfig.bZSSkeletonizing = false;  
    oConfig.strFilePrefix = "zsuen-ftc";  
    oConfig.iRepeat = 1;  
    oConfigs.add(oConfig);  
  
    oConfig = new Configuration();  
    oConfig.bBinarize = false;  
    oConfig.bZSCountouring = false;  
    oConfig.bZSFilling = true;  
    oConfig.bZSThinning = true;  
    oConfig.bZSSkeletonizing = true;  
    oConfig.strFilePrefix = "zsuen-fts-3";  
    oConfig.iRepeat = 3;  
    oConfigs.add(oConfig);  
  
    /*  
    oConfig = new Configuration();  
    oConfig.bBinarize = false;  
    oConfig.bZSCountouring = false;  
    oConfig.bZSFilling = true;  
    oConfig.bZSThinning = false;  
    oConfig.bZSSkeletonizing = true;  
    oConfig.strFilePrefix = "zsuen-fs-3";  
    oConfig.iRepeat = 3;  
    oConfigs.add(oConfig);  
    */  
  
    for(Configuration oRunConfig: oConfigs)  
    {  
        ident(oRunConfig);  
    }  
  
    break;  
}  
  
/*  
 * -----  
 * Training  
 * -----
```

```

*/
// Add a single sample to the training set
case OPT_SINGLE_TRAIN:
{
    throw new NotImplementedException();
}

// Train on a directory of files
case OPT_TRAIN:
case MARF.NLP.TRAIN:
{
    throw new NotImplementedException();
}

/*
 * -----
 * Training Set Data Display
 * -----
 */
case OPT_SHOW_TRAINING_SET_DATA:
{
    System.out.println(
    (
        marf.Classification.Classification.loadTrainingSet
        (
            marf.Storage.IStorageManager.DUMP_GZIP_BINARY,
            soGetOpt.getOption(OPT_DIR_OR_FILE)
        )
    );
    break;
}

/*
 * -----
 * Stats
 * -----
 */
case OPT_STATS:
{
    throw new NotImplementedException();
}

/*
 * Best Result with Stats
 */
case OPT_BEST_SCORE:
{
    throw new NotImplementedException();
}

/*
 * Reset Stats
 */
case OPT_RESET:
{
    throw new NotImplementedException();
}

/*
 * Versioning
 */
case OPT_VERSION:
{
    System.out.println("OCTMARF Application, v." + getVersion());
    System.out.println("Using MARF, v." + MARF.getVersion());
    validateVersions();
}

```

```
        break;
    }

    /*
     * Help
     */
    case OPT_HELP_SHORT:
    case OPT_HELP_LONG:
    {
        usage();
        break;
    }

    /*
     * Invalid major option
     */
    default:
    {
        throw new Exception("Unrecognized option: " + argv[0]);
    }
} // major option switch
} // try

/*
 * No arguments have been specified
 */
catch(ArrayIndexOutOfBoundsException e)
{
    System.err.println("No arguments have been specified.");
    System.err.println(e.getMessage());
    e.printStackTrace(System.err);

    usage();
}

/*
 * MARF-specific errors
 */
catch(MARFException e)
{
    System.err.println(e.getMessage());
    e.printStackTrace(System.err);
}

/*
 * Invalid option and/or option argument
 */
catch(Exception e)
{
    System.err.println(e.getMessage());
    e.printStackTrace(System.err);
    usage();
}

/*
 * Regardless whatever happens, close the db connection.
 */
finally
{
    try
    {
        Debug.debug("Closing DB connection...");
    }
    catch(Exception e)
    {
        Debug.debug("Closing DB connection failed: " + e.getMessage());
        e.printStackTrace(System.err);
        System.exit(-1);
    }
}
```

```

        }

    }

}

/***
 * Computes duration and outputs it as a string
 * @param plStartTime
 * @param plEndTime
 * @return String-formatted duration
 */
private static String getDuration(long plStartTime, long plEndTime)
{
    // XXX: constify
    int iOneSecInMs = 1000;
    int iOneMinInMs = 60 * iOneSecInMs;
    int iOneHourInMs = 60 * iOneMinInMs;
    int iOneDayInMs = 24 * iOneHourInMs;

    long lDuration = plEndTime - plStartTime;

    long lDays = lDuration / iOneDayInMs;
    long lModTimeLeft = lDuration % iOneDayInMs;

    long lHours = lModTimeLeft / iOneHourInMs;
    lModTimeLeft %= iOneHourInMs;

    long lMinutes = lModTimeLeft / iOneMinInMs;
    lModTimeLeft %= iOneMinInMs;

    long lSeconds = lModTimeLeft / iOneSecInMs;
    lModTimeLeft %= iOneSecInMs;

    long lMilliSeconds = lModTimeLeft;

    StringBuffer oDuration = new StringBuffer()
        .append(lDays + "d:" + lHours + "h:" + lMinutes + "m:" + lSeconds + "s:" + lMilliSeconds +"ms:" + lDuration + "ms")
        ;

    return oDuration.toString();
}

/***
 * Generic ident routine.
 * @throws Exception
 */
public static final void ident(Configuration poConfig)
throws Exception
{
    long lTimeStart = System.currentTimeMillis();
    {
        AScanLoader oLoader = new AScanLoader();

        // Process all .txt files in the directory
        File[] aoSampleFiles = new File("resources/data").listFiles();

        Binarizer oBinarizer = new Binarizer();
        ZhangSuenTransform oTransform = new ZhangSuenTransform();

        for(int i = 0; i < aoSampleFiles.length; i++)
        {
            String strFilename = aoSampleFiles[i].getPath();

            if(aoSampleFiles[i].isFile() && strFilename.toLowerCase().endsWith(DEFAULT_SAMPLE_FILE_EXTENSION))
            {
                long lSliceTimeStart = System.currentTimeMillis();

                // Load them one by one
                System.out.println("Loading " + strFilename + " into slice " + oLoader.sizeInSlices() + " of 3D volume.");
            }
        }
    }
}

```

```

oLoader.load(strFilename);

// Trial processing
{
    PPMDumper oDumper = new PPMDumper(poConfig.strFilePrefix + "." + i);

    if(poConfig.bBinarize == true)
    {
        oBinarizer.preprocess2D(oLoader.getVolume(), i);
    }

    if
    (
        poConfig.bZSCountouring == true
        ||
        poConfig.bZSFilling == true
        ||
        poConfig.bZSSkeletonizing == true
        ||
        poConfig.bZSThinning == true
    )
    {
        oTransform.setCountouring(poConfig.bZSCountouring);
        oTransform.setFill(poConfig.bZSFilling);
        oTransform.setSkeletonizing(poConfig.bZSSkeletonizing);
        oTransform.setThinning(poConfig.bZSThinning);

        for(int r = 0; r < poConfig.iRepeat; r++)
        {
            oTransform.detect2D(oLoader.getVolume(), i);
        }
    }

    System.out.print("Dumping " + oDumper.getFilename() + "... ");
    for(double[] adScanLine: oLoader.getDouble3DScan()[i])
    {
        oDumper.addToData(adScanLine);
    }

    // Save as a PPM
    oDumper.dump();
    System.out.println("Done.");
} // end trial processing

long lSliceTimeFinish = System.currentTimeMillis();
System.out.println
(
    "Slice processing and saving time: " +
    getDuration(lSliceTimeStart, lSliceTimeFinish)
);
} // if
}

long lTimeFinish = System.currentTimeMillis();
System.out.println
(
    "Total time volume took: " + getDuration(lTimeStart, lTimeFinish)
    + " for configuration: " + poConfig
);
}

/***
 * Displays application's usage information and exits.
 */
private static final void usage()
{
    System.out.println
(

```

```

"Usage:\n"
+ "    java OCTMARFApp      --train <samples-dir> [options]          -- train mode\n"
+ "                          --single-train <sample> [options]      -- add a single sample to the training set\n"
+ "                          --ident <sample> [options]           -- identification mode\n"
+ "                          --batch-ident <samples-dir> [options]   -- batch identification mode\n"
+ "                          --train-nlp [ --debug ] [ OPTIONS ] <language> <corpus-file>\n"
+ "                          --ident-nlp [ --debug ] [ OPTIONS ] foo <bar|corpus-file>\n\n"
+ "                          --debug                         -- include verbose debug output\n"
+ "                          --gui                           -- use GUI as a user interface\n"
+ "                          --stats=[per-config|per-writer|both] -- display stats (default is per-config)\n"
+ "                          --best-score                     -- display best classification result\n"
+ "                          --reset                         -- reset stats\n"
+ "                          --version                       -- display version info\n"
+ "                          --help | -h                      -- display this help and exit\n\n" + 

"Options (one or more of the following):\n\n" +
"\n

"Loaders:\n\n"
+ "    -wav             - assume WAVE files loading (default)\n"
+ "    -text            - assume loading of text samples\n"
+ "    -tiff            - assume loading of TIFF samples\n"
+ "\n" + 

"Preprocessing:\n\n"
+ "    -silence        - remove silence (can be combined with any of the below)\n"
+ "    -noise           - remove noise (can be combined with any of the below)\n"
+ "    -raw             - no preprocessing\n"
+ "    -norm            - use just normalization, no filtering\n"
+ "    -low             - use low-pass FFT filter\n"
+ "    -high            - use high-pass FFT filter\n"
+ "    -boost           - use high-frequency-boost FFT preprocessor\n"
+ "    -band            - use band-pass FFT filter\n"
+ "    -bandstop        - use band-stop FFT filter\n"
+ "    -endp            - use endpointing\n"
+ "    -lowcfe          - use low-pass CFE filter\n"
+ "    -highcfe         - use high-pass CFE filter\n"
+ "    -bandcfe         - use band-pass CFE filter\n"
+ "    -bandstopcfe    - use band-stop CFE filter\n"
+ "\n" + 

"Feature Extraction:\n\n"
+ "    -lpc             - use LPC\n"
+ "    -fft             - use FFT\n"
+ "    -minmax          - use Min/Max Amplitudes\n"
+ "    -randfe          - use random feature extraction\n"
+ "    -aggr            - use aggregated FFT+LPC feature extraction\n"
+ "    -f0               - use F0 (pitch, or fundamental frequency; NOT IMPLEMENTED)\n"
+ "    -segm            - use Segmentation (NOT IMPLEMENTED)\n"
+ "    -cepstral         - use Cepstral analysis (NOT IMPLEMENTED)\n"
+ "\n" + 

"Classification:\n\n"
+ "    -nn              - use Neural Network\n"
+ "    -cheb            - use Chebyshev Distance\n"
+ "    -eucl            - use Euclidean Distance\n"
+ "    -mink            - use Minkowski Distance\n"
+ "    -diff             - use Diff-Distance\n"
+ "    -zipf            - use Zipf's Law-based classifier\n"
+ "    -randcl          - use random classification\n"
+ "    -markov          - use Hidden Markov Models (NOT IMPLEMENTED)\n"
+ "    -hamming          - use Hamming Distance\n"
+ "    -cos              - use Cosine Similarity Measure\n"
+ "\n" + 

"NLP/Ngrams/Smoothing:\n\n"
+ "    -interactive     - interactive mode for classification instead of reading from a file\n"
+ "    -char            - use characters as n-grams (should always be present for this app)\n\n"
+ "    -unigram         - use UNIGRAM model\n"

```

```

+ " -bigram      - use BIGRAM model\n"
+ " -trigram     - use TRIGRAM model\n\n"
+ " -mle         - use MLE\n"
+ " -add-one     - use Add-One smoothing\n"
+ " -add-delta    - use Add-Delta (ELE, d=0.5) smoothing\n"
+ " -witten-bell - use Witten-Bell smoothing\n"
+ " -good-turing  - use Good-Turing smoothing\n" +
"\n"
+ " -spectrogram - dump spectrogram image after feature extraction\n"
+ " -graph        - dump wave graph before preprocessing and after feature extraction\n"
+ " <integer>    - expected subject ID\n"
+ "\n"
);

System.exit(0);
}

/**
 * Retrieves String representation of the application's version.
 *
 * @return version String
 */
public static final String getVersion()
{
    return MAJOR_VERSION + "." + MINOR_VERSION + "." + REVISION;
}

/**
 * Retrieves integer representation of the application's version.
 *
 * @return integer version
 */
public static final int getIntVersion()
{
    return MAJOR_VERSION * 100 + MINOR_VERSION * 10 + REVISION;
}

/**
 * Makes sure the applications isn't run against older MARF version. Exits
 * with 1 if the MARF version is too old.
 */
public static final void validateVersions()
{
    if(MARF.getDoubleVersion() < (0 * 100 + 3 * 10 + 0 + .6))
    {
        System.err.println(
            "Your MARF version (" + MARF.getVersion()
            + ") is too old. This application requires 0.3.0.6 or above."
        );

        System.exit(1);
    }
}

/**
 * Composes the current configuration of in a string form.
 *
 * @param pstrArgv
 *          set of configuration options passed through the command line;
 *          can be null or empty. If latter is the case, MARF itself is
 *          queried for its numerical set up inside.
 *
 * @return the current configuration setup
 */
public static final String getConfigString(String[] pstrArgv)
{

```

```

// Store config and error/successes for that config
String strConfig = "";

if(pstrArgv != null && pstrArgv.length > 2)
{
    // Get config from the command line
    for(int i = 2; i < pstrArgv.length; i++)
    {
        // We do NOT want numerical IDs
        try
        {
            Integer.parseInt(pstrArgv[i]);
        }
        catch(NumberFormatException e)
        {
            // Skip .xml file names
            if(pstrArgv[i].matches(".*\\.xml"))
            {
                continue;
            }

            strConfig += pstrArgv[i] + " ";
        }
    }
}
else
{
    // Query MARF for it's current config
    strConfig = MARF.getConfig();
}

return strConfig;
}

/**
 * Sets default MARF configuration parameters as normalization for
 * preprocessing, FFT for feature extraction, Euclidean distance for
 * training and classification with no spectrogram dumps and no debug
 * information, assuming WAVE file format.
 *
 * @throws MARFException
 */
public static final void setDefaultConfig() throws MARFException
{
    /*
     * Default MARF setup
     */
    MARF.setPreprocessingMethod(MARF.DUMMY);
    MARF.setFeatureExtractionMethod(MARF.FFT);
    MARF.setClassificationMethod(MARF.EUCLIDEAN_DISTANCE);
    MARF.setDumpSpectrogram(false);
    // MARF.setSampleFormat(MARF.WAV);
    // MARF.setSampleFormat(MARF.TEXT);
    MARF.setSampleFormat(MARF.CUSTOM);
    MARF.setSampleLoaderPluginClass(AnyToWAVLoader.class.getName());

    //Debug.enableDebug(false);
}

/**
 * Customizes MARF's configuration based on the options.
 *
 * @throws MARFException
 *          if some options are out of range
 */
public static final void setCustomConfig()
throws MARFException
{

```

```

ModuleParams oParams = new ModuleParams();

for
(
    int iPreprocessingMethod = MARF.MIN_PREPROCESSING_METHOD;
    iPreprocessingMethod <= MARF.MAX_PREPROCESSING_METHOD;
    iPreprocessingMethod++
)
{
    if(soGetOpt.isActiveOption(iPreprocessingMethod))
    {
        MARF.setPreprocessingMethod(iPreprocessingMethod);

        switch(iPreprocessingMethod)
        {
            // Endpointing did not respond well to silence removal
            // and the definition of RAW assumes none of that is done.
            // Endpointing also has some extra params of its own.
            case MARF.RAW:
            case MARF.ENDPOINT:

            case MARF.DUMMY:
            case MARF.HIGH_FREQUENCY_BOOST_FFT_FILTER:
            case MARF.HIGH_PASS_FFT_FILTER:
            case MARF.LOW_PASS_FFT_FILTER:
            case MARF.BANDPASS_FFT_FILTER:
            case MARF.BAND_STOP_FFT_FILTER:
            case MARF.HIGH_PASS_BOOST_FILTER:
            case MARF.BAND_PASS_CFE_FILTER:
            case MARF.BAND_STOP_CFE_FILTER:
            case MARF.LOW_PASS_CFE_FILTER:
            case MARF.HIGH_PASS_CFE_FILTER:
            {

                // Kludge
                if(soGetOpt.isActiveOption(OPT_SILENCE_NOISE_REMOVAL))
                {
                    oParams.addPreprocessingParam(true);
                    oParams.addPreprocessingParam(true);
                }
                else
                {
                    // Normalization and filters seem to respond better
                    // to silence removal.
                    // The setting of the third protocol parameter
                    // (silence threshold)
                    // is yet to be implemented here.
                    oParams.addPreprocessingParam(soGetOpt.isActiveOption(OPT_NOISE_REMOVAL));
                    oParams.addPreprocessingParam(soGetOpt.isActiveOption(OPT_SILENCE_REMOVAL));
                }
            }

            break;
        }

        default:
        {
            assert false : "Not implemented valid preprocessing configuration parameter: " + iPreprocessingMethod;
        }
    } // switch

    break;
}
}

for
(
    int iFeatureExtractionMethod = MARF.MIN_FEATUREEXTRACTION_METHOD;
    iFeatureExtractionMethod <= MARF.MAX_FEATUREEXTRACTION_METHOD;
    iFeatureExtractionMethod++
)

```

```

        }

    if(soGetOpt.isActiveOption(iFeatureExtractionMethod))
    {
        MARF.setFeatureExtractionMethod(iFeatureExtractionMethod);

        switch(iFeatureExtractionMethod)
        {
            case MARF.FFT:
            case MARF.LPC:
            case MARF.RANDOM_FEATURE_EXTRACTION:
            case MARF.MIN_MAX_AMPLITUDES:
            case MARF.F0:
            case MARF.CEPSTRAL:
            case MARF.SEGMENTATION:
                // For now do nothing; customize when these methods
                // become parameterizable.
                break;

            case MARF.FEATURE_EXTRACTION_AGGREGATOR:
            {
                // For now aggregate FFT followed by LPC until
                // it becomes customizable
                oParams.addFeatureExtractionParam(new Integer(MARF.FFT));
                oParams.addFeatureExtractionParam(null);
                oParams.addFeatureExtractionParam(new Integer(MARF.LPC));
                oParams.addFeatureExtractionParam(null);
                break;
            }

            default:
                assert false;
        } // switch

        break;
    }
}

for
(
    int iClassificationMethod = MARF.MIN_CLASSIFICATION_METHOD;
    iClassificationMethod <= MARF.MAX_CLASSIFICATION_METHOD;
    iClassificationMethod++
)
{
    if(soGetOpt.isActiveOption(iClassificationMethod))
    {
        MARF.setClassificationMethod(iClassificationMethod);

        switch(iClassificationMethod)
        {
            case MARF.NEURAL_NETWORK:
            {
                // Dump/Restore Format of the TrainingSet
                oParams.addClassificationParam(TrainingSet.DUMP_GZIP_BINARY);

                // Training Constant
                oParams.addClassificationParam(0.5);

                // Epoch number
                oParams.addClassificationParam(20);

                // Min. error
                oParams.addClassificationParam(0.1);

                break;
            }
}

```

```

        case MARF.HAMMING_DISTANCE:
    {
        // Dump/Restore Format
        oParams.addClassificationParam(TrainingSet.DUMP_GZIP_BINARY);

        // Type of hamming comparison
        oParams.addClassificationParam(HammingDistance.STRICT_DOUBLE);

        break;
    }

    case MARF.MINKOWSKI_DISTANCE:
    {
        // Dump/Restore Format
        oParams.addClassificationParam(TrainingSet.DUMP_GZIP_BINARY);

        // Minkowski Factor
        oParams.addClassificationParam(6.0);

        break;
    }

    case MARF.EUCLIDEAN_DISTANCE:
    case MARF.CHEBYSHEV_DISTANCE:
    case MARF.MAHALANOBIS_DISTANCE:
    case MARF.RANDOM_CLASSIFICATION:
    case MARF.DIFF_DISTANCE:
    case MARF.MARKOV:
    case MARF.ZIPFS_LAW:
    case MARF.COSINE_SIMILARITY_MEASURE:
    {
        // Dump/Restore Format
        oParams.addClassificationParam(TrainingSet.DUMP_GZIP_BINARY);

        // For now do nothing; customize when these methods
        // become parameterizable.
        break;
    }

    default:
        assert false : "Unrecognized classification module";
    } // switch

    // Method is found, break out of the look up loop
    break;
}
}

// Assign meaningful params only
if(oParams.size() > 0)
{
    MARF.setModuleParams(oParams);
}
}

// EOF

```

A.4 PPM Dumper

```

package marf.apps.oct.OCTMARF.Storage;

import java.io.BufferedOutputStream;
import java.io.DataOutputStream;
import java.io.FileOutputStream;
import java.util.Vector;

```

```

import marf.Storage.StorageException;
import marf.util.Debug;


/*
 * <p>Dumps an image to a PPM file.</p>
 *
 * @author Serguei Mokhov
 * @version $Id: PPMDumper.java,v 1.5 2012/01/02 08:06:33 mokhov Exp $
 * @since 0.0.1
 */

public class PPMDumper
{
    /**
     * The data vector.
     */
    protected Vector<Double[]> oData = null;

    /**
     * Current minimum.
     */
    protected double dMin = 0.0;

    /**
     * Current maximum.
     */
    protected double dMax = 0.0;

    /**
     * To differentiate file names based on the feature extraction method name.
     */
    protected String strMethod = "";

    /**
     * Constructor.
     */
    public PPMDumper()
    {
        this.oData = new Vector<Double[]>();
    }

    /**
     * Constructor with a feature extraction method name.
     * @param pstrMethodName String representing FE module name
     */
    public PPMDumper(String pstrMethodName)
    {
        this();
        this.strMethod = pstrMethodName;
    }

    /**
     * Dumps image.
     * @throws StorageException
     */
    public final void dump()
    throws StorageException
    {
        try
        {
            Debug.debug("Dumping image " + this.strMethod + ".ppm");
            Debug.debug(".dump() - data size in vectors: " + this.oData.size());

            FileOutputStream oFOS = null;
            DataOutputStream oOutFile = null;

            // oFOS = new FileOutputStream("58." + this.strMethod + ".ppm");
            // oFOS = new FileOutputStream("58.ppm");
        }
    }
}

```

```

oFOS = new FileOutputStream(this.strMethod + ".ppm");
//oOutFile = new DataOutputStream(oFOS);
oOutFile = new DataOutputStream(new BufferedOutputStream(oFOS));

// Output PPM header
/*
man ppm:
    - A "magic number" for identifying the file type. A pgm file's magic number is the two characters "P6".
    - Whitespace (blanks, TABs, CRs, LFs).
    - A width, formatted as ASCII characters in decimal.
    - Whitespace.
    - A height, again in ASCII decimal.
    - Whitespace.
    - The maximum color value (Maxval), again in ASCII decimal. Must be less than 65536.
    - Newline or other single whitespace character.
    - A raster of Width * Height pixels, proceeding through the image in normal English reading order. Each pixel is a
        green, and blue samples, in that order. Each sample is represented in pure binary by either 1 or 2 bytes. If
        than 256, it is 1 byte. Otherwise, it is 2 bytes. The most significant byte is first.
*/
// Output data

// Make max be at 75%
this.dMax = 255;

int iWidth = this.oData.size();
int iHeight = this.oData.elementAt(0).length;

oOutFile.writeBytes
(
    "P6\n"
    + iWidth + "\n"
    + iHeight + "\n"
    + "255\n"
);

for(int i = iHeight - 1; i >= 0; i--)
{
    for(int j = 0; j < iWidth; j++)
    {
        Double[] adData = this.oData.elementAt(j);

        // Colors, RGB, hence 3
        for(int m = 0; m < 3; m++)
        {
            oOutFile.writeByte(adData[i].byteValue());
        }
    }
}

oOutFile.flush();

Debug.debug
(
    "Done dumping image " +
    this.strMethod +
    ".ppm [" + (this.oData.size() * iHeight * iWidth) + " bytes]"
);
}
catch(Exception e)

```

```

    {
        throw new StorageException(e);
    }
}

public void addToData(double[] padData)
{
    Double[] oNewData = new Double[padData.length];
    //Arrays.copy(oNewData, padData);

    for(int i = 0; i < padData.length; i++)
    {
        oNewData[i] = padData[i];
    }

    this.oData.add(oNewData);
}

public void addToData(Double[] pData)
{
    this.oData.add(pData);
}

/**
 * @return the oData
 */
public Vector<Double[]> getData()
{
    return this.oData;
}

/**
 * @param oData the oData to set
 */
public void setData(Vector<Double[]> poData)
{
    this.oData = poData;
}

public String getFilename()
{
    return this.strMethod;
}
}

// EOF

```

Index

API

AScanLoader, 18, 26
Binarizer, 19, 20
BMPDumper, 18
Configuration, 19, 20
Detector, 19
double, 17, 18
FabritiusILMDetector, 19
IDetector, 19
IPreprocessor, 19
IProcessor, 19
marf.apps.oct.OCTMARF.framework.a2, 17
MARFCATApp, 17
OCTMARFApp, 17, 18, 30
PPMDumper, 18, 47
Preprocessor, 19
short, 17, 18
String, 17, 18
Volume, 17, 18, 28
WriterIdentApp, 17
ZhanSuenTransform, 19

C++, 15

Files

data.zip, 9
pic.zip, 9

Frameworks

MARF, 15, 18

GIPSY, 15

Java, 15

Libraries

MARF, 15, 18

MARF, 15, 18

Tools

volview, 15